PREVENTING DELAYED CRACKS IN DEEP DRAWING
PROCESSES OF SUS304 CYLINDRICAL CUPS USING A COATED
DIE

PHOO YOONG HAU

SUBMITTED TO THE

FACULTY OF ENGINEERING UNIVERSITY OF MALAYA

IN PARTIAL FULFILMENT OF THE REQUIREMENTS FOR

THE DEGREE OF MASTER OF MECHANICAL ENGINEERING

2019

PREVENTING DELAYED CRACKS IN DEEP DRAWING PROCESSES OF
SUS304 CYLINDRICAL CUPS USING A COATED DIE

ABSTRAK

Retakan longitudinal yang tertunda cenderung membentuk di sepanjang dinding yang ditarik sepenuhnya SUS304 keluli tahan karat dengan serta-merta selepas proses penarik dalam untuk tempoh inkubasi tertentu dari beberapa minit hingga beberapa hari. Walaupun retakan yang tertunda telah dihapuskan dengan dai yang digilap dan tidak bersalut menggunakan pelincir nano di bawah Blank holding force (BHF) dalam kajian sebelumnya, rentang BHF bebas retakan terlalu sempit dan magnitudnya terlalu tinggi. Dalam kajian ini, rentang BHF bebas retak telah berjaya dikurangkan dari 29kN-31kN kepada 5kN-10kN menggunakan dai yang bersalut Titanium Nitride (TiN) di bawah pelinciran konvensional. Kepekatan martensit yang disebabkan oleh ubah bentuk yang tinggi di titik lembah yang bertebaran di sepanjang pinggan cawan yang dihasilkan daripada tegasan mampatan tinggi yang mengelilingi semasa proses penarik dalam meningkatkan peluang untuk retakan yang tertunda. Penghapusan retakan yang tertangguh adalah disebabkan oleh pengurangan jumlah penebalan dinding, peningkatan dalam ketinggian lembah dan tegasan sisa tegangan lenturan yang rendah di sepanjang tepi cawan. Hasil eksperimen menunjukkan bahawa retakan yang tertunda diperhatikan dalam cawan yang dibentuk dengan dai yang digilap dan tidak bersalut apabila purata penebalan dinding di lembah lembah melebihi 33.5% dalam had BHF dari 5kN-15kN. Retak telah dicegah untuk 28% penebalan dinding di bawah BHF daripada 12kN menggunakan dai yang sama. Bagaimanapun, tidak ada retakan tertunda yang diperhatikan dalam cawan yang dibentuk dengan TiN bersalut mati dalam had BHF dari 5kN-10kN. Kerana purata penebalan dinding di titik lembah dari cawan ini berkisar dari 24.5% hingga 32.7%, lebih rendah daripada had penebalan dinding untuk retak iaitu 33.5%. Ketinggian lembah yang lebih daripada 33mm untuk dai bersalut dan dai tidak bersalut membuat cawan bebas dari retakan tertunda, manakala cawan lain dengan ketinggian lembah yang lebih rendah daripada 33mm mengalami retakan tertunda. Dai bersalut TiN mempunyai kekasaran permukaan rata-rata yang lebih rendah ($Ra = 0.382\mu m$) daripada dai tidak bersalut yang digilap ($Ra = 0.581\mu m$), memberikan laluan daya geseran yang lebih rendah untuk aliran bahan kosong ke pemanjangan dai dan terbesar yang mungkin. Selain itu, nilai BHF yang kecil sentiasa diingini sebagai risiko yang lebih tinggi untuk patah cawan dengan nilai BHF yang lebih besar. Rangkaian BHF bebas terlewat dikehendaki kerana bahagian itu boleh dibentuk dengan mana-mana nilai BHF dalam rentang untuk mencapai matlamat yang diinginkan.

Kata kunci: Keluli tahan karat metastable, Prosess penarik dalam, Retak tertunda, dai yang bersalut Titanium Nitride

PREVENTING DELAYED CRACKS IN DEEP DRAWING PROCESSES OF SUS304 CYLINDRICAL CUPS USING A COATED DIE

ABSTRACT

Longitudinal delayed cracks tend to form along the sidewall of fully drawn SUS304 metastable austenitic stainless steel cylindrical cups immediately after the deep drawing process for a certain incubation period ranging from several minutes to several days. Although the delayed cracks were eliminated with a polished and uncoated die using nano-lubrication under elevated blank holding forces (BHF) in a previous study, the crack-free BHF range was too narrow and the magnitude was too high. In this study, the crack-free BHF range has been successfully reduced from 29kN-31kN to 5kN-10kN using a Titanium Nitride (TiN) coated drawing die under conventional lubrication. The high concentration of deformation-induced martensite in the thickened valley points along the cup edge resulting from the high circumferential compressive stress during the drawing process increases the chances for the delayed cracks. The elimination of the delayed cracks was attributed to the reduce in amount of wall thickening, increase in valley heights and the low circumferential tensile residual stress along the cup edge. The experimental results showed that delayed cracks were observed in cups formed with the polished and uncoated die when the average amount of wall thickening in the valley points exceeded 33.5% within the BHF limits from 5kN-15kN. The cracks were prevented for 28% of wall thickening under the BHF of 12kN using the same die. However, no delayed cracks were observed in the cups formed with the TiN coated die within the BHF limits from 5kN-10kN. Because the average amount of wall thickening in the valley points of these cups ranged from 24.5%-32.7%, lower than the wall thickening limit for crack i.e. 33.5%. The valley height that more than 33mm for coated and uncoated die make the cup free from delayed crack, while the other cup with valley height lower than 33mm were suffer from delayed crack. The TiN-coated die has a lower average surface roughness (R_a=0.382µm) than the polished uncoated die (R_a=0.581µm), provides a lower frictional force path for the flow of blank material into the die and largest elongation as possible. Besides that, the small BHF values were always desired as the higher risk for fracture of the cup with larger BHF value. The widest crack free BHF range was desired due to the part can be formed with any values of BHF within the range in order to achieve desired objectives.

Keywords: Metastable stainless steel, Deep drawing, Delayed crack, TiN coated die

ACKNOWLEDGMENT

It is always a pleasure to remind the fine people in the UNIVERSITY OF MALAYA for their sincere guidance that I received to uphold my Master's Degree study.

Foremost, I would like to express my sincere gratitude to my advisor Dr. Tan Chin Joo for the continuous support of my research, for his patience, motivation, enthusiasm, and immense knowledge. His guidance helped me in all the time of research and writing of this thesis. I could not have imagined having a better advisor and mentor for my research project.

Secondly, I would like to thank my parents, for giving birth to me in the first place and supporting me spiritually throughout my life.

Finally, I apologize to all other unnamed who help me in various ways to have good training.

TABLE OF CONTENTS

LIST OF FIGURE

LIST OF TABLE

LIST OF SYMBOLS AND ABBREVIATIONS

BHF   -   BLANK HOLDING FORCE

CVD   -   CHEMICAL VAPOR DEPOSITION

DLC   -   DIAMOND LIKE CARBON

EDM   -   ELECTRICAL DISCHARGE MACHINING

LDR   -   LIMITING DRAW RATIO

LVDT   -   LASER DISTANCE SENSOR

PVD   -   PHYSICAL VAPOR DEPOSITION

TiC   -   TITANIUM CARBIDE

TiN   -   TITANIUM NITRIDE

Chapter 1 INTRODUCTION

1.1   Background

Stainless steel products such as kitchen sinks, containers, and some automotive parts are formed with deep drawing processes from thin SUS304 sheets. However, delayed (or longitudinal) cracks tend to form along the sidewall of drawn cups after several minutes, hours or days immediately after the drawing process. In the previous study by Tan, Ibrahim, & Muhamad (2018), the cracks were successfully eliminated with an increase in Blank Holding Force (BHF) ranging from 3.6 to 3.9 times of the minimum pressure that needed to suppress the wrinkle aided by nano-lubrication using a polished and uncoated die.

In this study, the effect of die coating on eliminating the delayed cracks under the elevated BHF without applying the nano-lubricant is investigated in an experiment at its Limiting Drawing Ratio (LDR). The crack-free BHF range using the coated die with a commercial lubricant is determined. The change in tensile residual hoop stresses and the deformation behaviors of the cups in relation to the elimination of the cracks were characterized.

1.2   Problem Statements

The content of internal hydrogen in the blank material, deformation-induced martensite and tensile residual hoop stresses will cause the delayed cracks on deep-drawn SUS304 cylindrical cups. The tiny amount of hydrogen is accumulated during the steel making process and it is inevitable in the production. Although the internal hydrogen can be removed by the costly annealing process, it is not attractive to do so.

The cup edge is subject to the highest amount of compressive stress during the deep drawing process, resulting in an increase in wall thickness. Therefore, the concentration of the deformation-induced martensite is the highest along the cup edge, leading to an increase in the risk of the cracks. Reducing the degree of wall thickening along the cup edge with elevated BHF will lower the concentration of the deformation-induced martensite and the risk of crack.

Die coating is widely used to enhance the tool life and its tribological performance. The effect of using die coating on lowering the degree of wall thickening along the cup edge and the tensile residual hoop stress under the high BHF will be investigated. The extreme pressure performance of the boundary layer in the contact surface will enhance the flow of material from the thick portion, resulting in a lower degree of wall thickening. The risk of the cracks can be reduced with the lower degree of wall thickening due to the high compression.

1.3   Objectives

1. To determine the crack-free BHF range for deep drawn SUS304 cups using a coated die
2. To investigate the change in deformation and the change in tensile residual hoop stress under the elevated BHF using the coated die
3. To explain the elimination of the formation of the delayed cracks under the elevated BHF for the coated die.

1.4   Scope

This study is focused on delayed cracks phenomena for deep drawn SUS304 cylindrical cups. In this study, a die coated with Titanium Nitride (TiN) will be used to prevent delay crack. In addition, the crack-free BHF range using the coated die with a commercial lubricant is determined. The residual stress under the elevated BHF using the coated die will be measured and calculated using the ring slitting method.

1.5   Limitations

This research is limited to the delayed cracks phenomena in deep drawing processes of SUS304 cylindrical cups because SUS304 stainless steel is a very common stainless steel in the industry. Other less common stainless steels such as SUS316 and SUS430 are not included in this research. Other austenite stainless steels such as SUS 302, SUS 305, SUS 308 and SUS 309 are not included in this research as well, due these grades of stainless steel are not common for metal stamping.

The coated die in this research will be limited to TiN coating only. Another common coating such as diamond-like carbon (DLC), Titanium Carbide (TiC) is not included in this research.

The deep drawing process is performed at room temperature, not at elevated temperature as production cost will increase resulting from the high cost of heating. In addition, this research only deep drawn cup at its LDR will be investigated, because the delayed crack most likely will occur at LDR. The LDR is maintaining at 2.12.

The residual stress will be measured and calculated using the ring slitting method, another famous method such as X-ray diffraction method will not include in the research. In addition, the analysis of internal hydrogen and deformation-induced martensite will not include in the research as well.

1.6   Significant of research

This research explains mechanism the elimination and the formation of the delayed cracks under the elevated BHF for the TiN coated die. As it is one of the methods to eliminate or reduce the risks of formation of the delayed crack of deep drawn SUS304 cylindrical cups.

Chapter 2 LITERATURE REVIEW

2.1   Deep Drawing Process

Deep drawing is one of the widely used sheets metal forming operations. The part produced by deep-drawing is known as a deep-drawn cup with the depth is at least half of its diameter. Figure 2.1 shows some products produced by the deep drawing process.

Figure 2.1: Deep drawn product

A flat blank is shaped into a cylindrical cup by forcing a punch against the center portion of a blank that rests on the die ring. The flow of flat blank into the die cavity is controlled by BHF. The material is drawn out of the blank holder-die region during the forming stage and the material is subjected to compressive and tensile stresses in this portion. Figure 2.2 shows the schematic diagram of deep drawing.
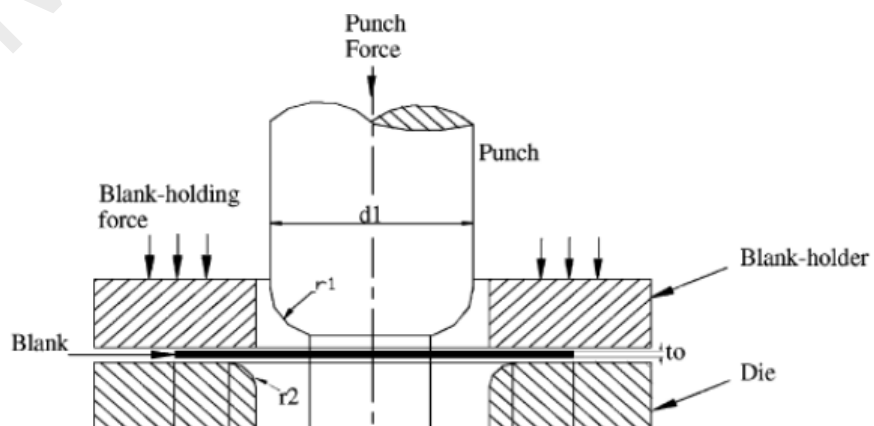
Figure 2.2: Deep drawing

2.2 Common Defect in Deep Drawing

There three major common defects which can be found in deep drawing process including fracture, wrinkling, and earing (Swapna, Rao, & Radhika, 2018).

When the sheet metal is subjected to strains exceeding its limits, fracture of the cup bottom will occur. This is due the maximum forming load appears at the cup bottom and also stress concentration lines are converging in this section. Once this necking exceeds beyond a certain value, fracture appears in the drawn cup. A formed cup with a fracture at the cup bottom is shown in Figure 2.3.

Figure 2.3: Fracture in deep drawing (Swapna et al., 2018)

when compressive stresses in the circumferential direction at the flange portion reach a critical point of instability, wrinkling will occur. It can occur in regions where the workpiece is unsupported or when the BHF is insufficient. The wrinkling can be prevented by increasing BHF, however, the excessing BHF will cause tearing. Wrinkling and tearing defects are shown in Figure 2.4.
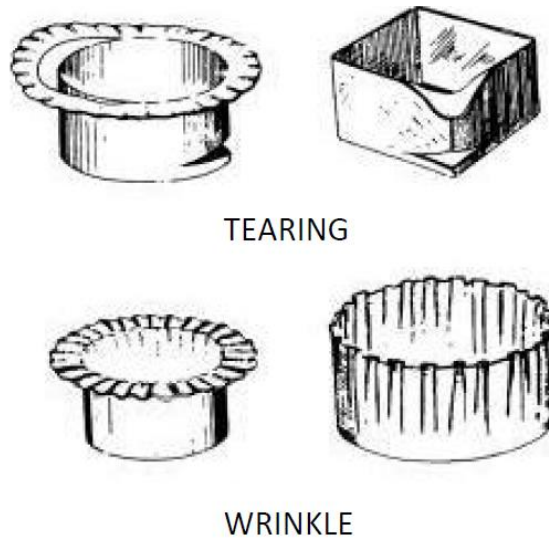
Figure 2.4: Tearing and wrinkling in deep drawn cup (S. H. Kim, Kim, & Huh, 2001)

A deep-drawn cup with an uneven top edge is caused by the anisotropic properties of the blank material. For example, ears are formed at the top as shown in Figure 2.5. This defect is called earing and it is because of planar anisotropy of the blank material. Anisotropic behavior refers to the direction dependence of mechanical properties. Tajally, Emaddodin, & Qods (2011) stated that metals have undergone extensive plastic deformation, show anisotropy behavior in mechanical properties and plastic deformation in different directions due to preferred grain orientation at the structure. According to Trzepieciński & Gelgele (2011), there are two types of anisotropy parameter including normal and planar anisotropy. In normal anisotropy the properties differ in the thickness direction; in planar anisotropy however, the properties vary with the orientation in the plane of the sheet. Whereas draw-ability of sheets increases with normal anisotropy, planar anisotropy leads to the formation of ears in the cup.
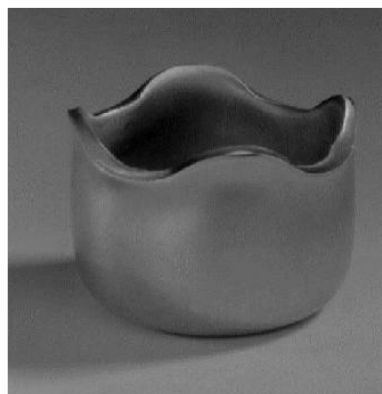
Figure 2.5: Earing in deep drawing (Swapna et al., 2018)

2.3 Stainless Steel

The iron-based alloy with a minimum of 10.5% is known as stainless steel. Due to the alloying chromium, stainless steel has good resistance to corrosion. A thin passive layer of chromium oxide on the stainless steel surface due to the reaction between chromium and oxygen in the air, this passive layer has very high oxidation resistance. In addition, the passive layer able to selfheal, which means that the scratched surface will cover back by new chromium oxide formed in the scratch, and thus protect the stainless steel from corrosion. There are many different grades of stainless steel with a variety of properties. They are five main different stainless steel which named after their structure:

1. Ferritic - SUS409, SUS410L, SUS430 and etc.
2. Martensitic – SUS410, SUS416, SUS420 and etc.
3. Austenitic – 300 series and 200 series
4. Austenitic and Ferritic (Duplex) – 2101, 2102,2202,2304 and etc.
5. Precipitation hardening

2.3.1 Austenitic Stainless Steels and Metastable Austenitic Stainless Steel

Michler (2015) stated that greater corrosion resistance and impressive mechanical properties are one of the important properties for austenitic stainless steels. This type of stainless steel is named after their primary crystalline structure which is known as austenite. These additions of the nickel, manganese and nitrogen (also know as austenite stabilizing elements) will aid in the formation of austenite crystalline structure.

Austenitic stainless steel has two main subgroups, which known as 200 series and 300 series. The addition of nickel will aid 300 series austenitic stainless steel to form austenitic structure, while 200 series stainless steel is achieved austenite by the addition of manganese, nitrogen and a very small amount of nickel. SUS304 austenitic stainless steel with low-nickel composition is the most common austenitic stainless steel. SUS304 austenitic stainless steel is the most common raw material for cookware products, cutlery products, and kitchen equipment.

Generally, the traditional austenitic stainless steels have a chemical composition of 18% and 8% of chromium and nickel respectively. In addition, during the deformation process such as deep drawing, SUS304 will transform into the martensitic phase. This might due to the thermodynamic properties of the austenite phase is unstable at room temperature. As seen in the phase diagram in Figure 2.6 the phases expected at room temperature (in true equilibrium) are austenite (γ), ferrite (α) and carbides.
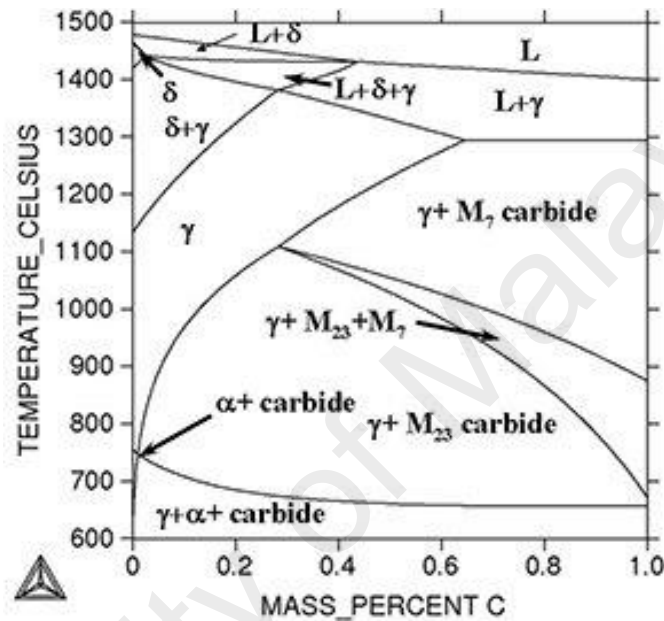
Figure 2.6: Equilibrium phase diagram of type 18-8 austenitic stainless steel with carbon as a variable (Nilsson, 2017)

However, usually, the commercial materials will not be used under their equilibrium state. Metastable austenitic stainless steels are stainless steel that makes use of the properties of strain-induced α'-martensite formed during deformation (Nilsson, 2017). While Kim, & Lee (2004) defined metastable austenitic stainless steels as the group of stainless steel in which under deformation the austenitic microstructure will transform readily into martensite.

Papula, Talonen, & Hänninen (2014) state that metastable austenitic stainless steels with the partly transformation of austenite microstructure into martensite microstructure under deformation or plastic strain, resulting in an excellent combination of strength and elongation.

Applications of metastable austenitic stainless steel widely used in the automotive industry such as windshield wipers, brake springs, seat belt retractors and valve springs. Metastable austenitic stainless steels also widely used as raw material for contact springs, hinge springs and clamp springs in electric connectors.

2.4   Delayed Cracking

Papula et al. (2015) stated that delayed cracking is a mechanism where a subcritical crack produces time-delayed cracking which there is even no external stress applied to the formed components. According to research that has done by Zinbi & Bouchou (2010), delayed cracking is attribute to internal hydrogen content of the material, residual stresses, strain-induced α'-martensitic transformation and chemical composition of the material. Besides that, Guo & Bleck (2016) stated that delayed cracking is also affected by forming parameters, such as drawing ratio, forming rate and forming temperature, since these process-related parameters influence the strain, residual stress as well as phase transformation in the deep drawn cups.

2.4.1   Strain-induced α'-martensitic transformation

Austenitic stability is the most important characteristic of the austenitic phase. Same with carbon steels, stainless steels with metastable austenite are thermodynamically unstable which tend to transform into martensite either by cold work deformation such as deep drawing. Michler (2015) stated that the starting temperature of martensite for commercial alloys is well below room temperature, but during normal manufacturing processing such as cold rolling, deep drawing, wire drawing, grinding, or polishing the strain-induced α'-martensitic transformation is nearly to present. (Michler, 2015).

The strain-induced α'-martensitic transformation affected by many factors, such as the chemical composition of the steel, with Nickel, Chromium, Carbon, and Nitrogen having a strong effect (Berrahmoune, Berveiller, Inal, & Patoor, 2006). This may due to the close relation between Nickel composition and stability and stacking fault energy of austenite. Austenitic stability promotes cross slip and, thus reduces planar slip participation in fracture to favor a macroscopically more ductile appearance.

The research done by Wu & Huang (2015) shown that the increases in plastic strain will increase the martensitic phase content. The phase transformation resulting in the changes in the microstructure of grains. The material with the martensitic phase has higher strength and less ductility, this might due to the raises of resistance to the dislocation motions.

Lo, Shek, & Lai, (2009) and Maksimkin (1997) explained that there are two different types of martensite phases that can be found in austenitic stainless steels including hexagonal close-packed ε-martensite and body-centered cubic α'-martensite. The ε-martensite is an intermediate phase, which that reaches its highest volume fraction at relatively low strains and eventually transforms to α'-martensite at higher strains, so that at higher strains only α'-martensite is observed.

Berrahmoune et al. (2006) stated that the martensitic transformation will be resulting delayed cracking phenomenon, especially in the deep drawing process. Tan et al. (2018) stated that the risk of delayed cracking to occur became higher when the concentration of strain-induced α'-martensitic increases. The research done by Papula et al. (2014) shown that the delayed cracking that occurs in austenitic stainless steels deep drawn cup with the 5ppm or less internal hydrogen concentrations is close related to the presence of α'-martensite.

2.4.2 Effect of Hydrogen

According to Huang & Altstetter (1991), there is a small amount of hydrogen inside the metastable stainless steels and delayed cracked is appear due to this small amount of hydrogen. Hydrogen can enter into steel during its manufacturing process. For example, the water content in the raw materials or in the furnace gases, during pickling in mineral acids or cathodic cleaning, or during bright annealing.

Hydrogen embrittlement sensitivity is attributed to the stability of austenite, which means the larger the strain-induced α'-martensite content the higher the risk for fracture. This might due to the hydrogen embrittlement sensitivity of the martensitic microstructure is more sensitive than the austenitic microstructure. The kinetics of hydrogen embrittlement is limited by diffusion of hydrogen, due to the body center cubic phase has the higher hydrogen, body center cubic phase α'-martensite may act as a suitable medium for transport of hydrogen within the solid and may also medium for crack propagation. (Papula et al., 2015).

Bak, Abro, & Lee (2016) stated that α'-martensite transformation is closely related to hydrogen embrittlement. Thus the application of austenitic stainless steel such as SUS301, SUS304, and SUS316 in hydrogen-containing environments is limited due to α'-martensite acts as a good medium for the diffusion of hydrogen.

2.4.3 Residual Stress

In the deep drawing process, the flat circular blank is shaped into a cylindrical cup. The flat circular blank is placed over the die and a moving punch is then pushed the flat circular blank into the die cavity. As the punch moves downward, the edge of the blank (also known flange) moves radially inward. Thus, deformation mainly occurs in this portion. During the deep drawing process, there are three different stress subjected to the blank as shown in Figure 2.7.

At the flange portion where the primary deformation takes place, there are radial tension and circumferential compression is subjected to the flange of the cup. As a result, there is a wall thickening effect that takes place in the flange portion. The second deformation zone is the bending around the die radius while the third deformation zone is the uni-axial stretching (plane strain) in the cup wall, which causes thinning of the metal. There is only very little stress subjected to the punch; therefore the change in wall thickness of this portion is the lowest.
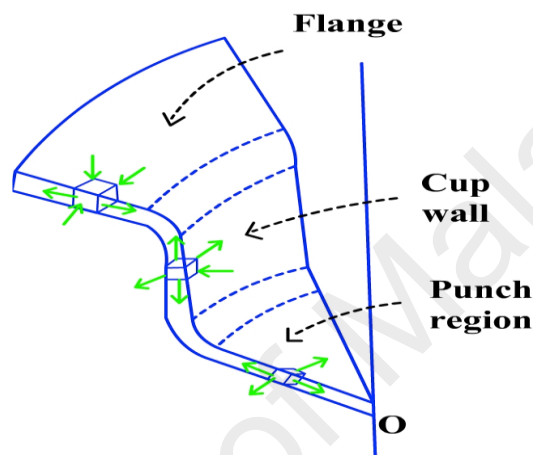
Figure 2.7: Stress in deep drawn cup

El Sherbiny, Zein, Abd-Rabou, & El shazly (2014) define residual stresses are stresses that remain in a solid material after the original cause of the stresses has been removed. The magnitude of residual stresses in a formed component increase as strain-induced α'-martensitic transformation increases. Thus, the α'-martensite phase has a higher concentration of residual stress than the austenite phase.

The residual stresses due to non-uniform plastic deformation, the maximum value of residual stress can go up to value that same with the yield stress of the material. According to Danckert (1995), the residual stresses can become very large for the deep drawing of austenitic stainless steel blank and cause the appearance of delayed crack. These stresses are tensile at the cup outer surface and compressive at the inner surface. From Figure 2.8, the maximum residual stresses can be found at the valley points located along the edge of the deep-drawn cup; therefore, the delayed crack first appears and propagates from this point.
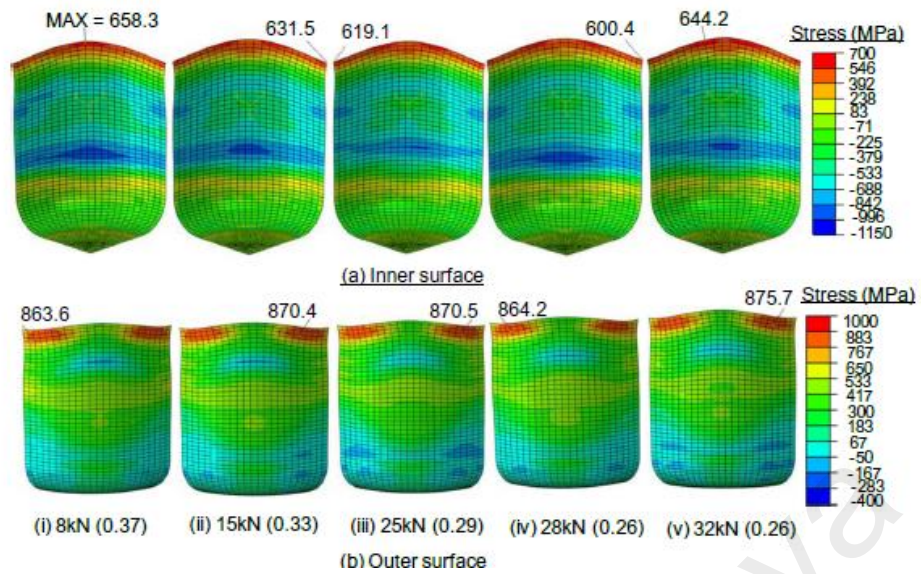
Figure 2.8: Residual hoop stresses at the inner and outer surfaces of deep-drawn cups obtained from simulation (Tan et al., 2018)

Tan & Aslian (2019) stated that due to a high concentration of residual stress, the valley points have a higher risk for the delayed cracks to occur. In the simulation results shown in Figure 2.9, the significant increase from compressive to tensile stress at the valley points during the tool separation stage. After the tools separate from the deep drawn cup, the stress increases significantly at the valley point. The compressive stress tends to transform into a high magnitude of tensile stress. The significantly increase in hoop stress after tools being separated from the deep drawn cup, the valley points have a higher risk for delayed crack.
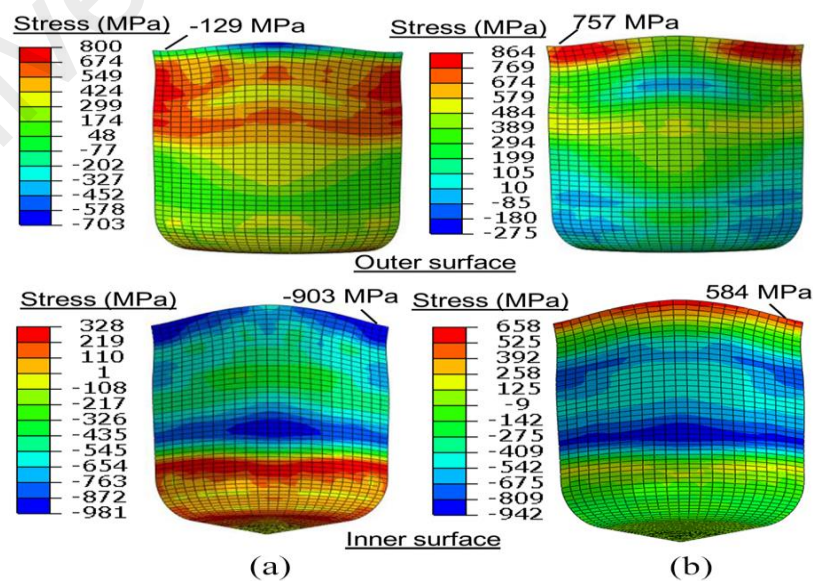
Figure 2.9: Hoop stress distribution at inner and outer surfaces of the cup at end of drawing stages (a) and tool separation stages (b) (Tan & Aslian , 2019)

2.4.4 Temperature

According to Kala (2017), the formability of the materials will become greater if the deep drawing process takes place at elevated temperatures (above the recrystallization temperature of material) which deformation will become easier. This might due to the high temperature will significantly decrease flow stresses and residual stress relief effect. The decrease of flow stress allows more stretching in the final products and deeper drawing.

Guo & Bleck (2016) increase the deep-drawn temperature from room temperature to 80°C, the martensitic transformation was strongly suppressed. As a result, delayed cracking was prevented by high-temperature forming. By increasing the forming rate, the martensitic transformation was suppressed due to adiabatic heating, which also shuns delayed cracking.

2.4.5 Drawing Ratio

The relationship between the initial blank diameter and the punch diameter is known as the drawing ratio. If the draw ratio is too large, the material does not flow and may stretch extensively. Successful deep draws have minimal stretching because the displacement of material is primarily in compression. Figure 2.10 shows the schematic diagram for the drawing ratio.
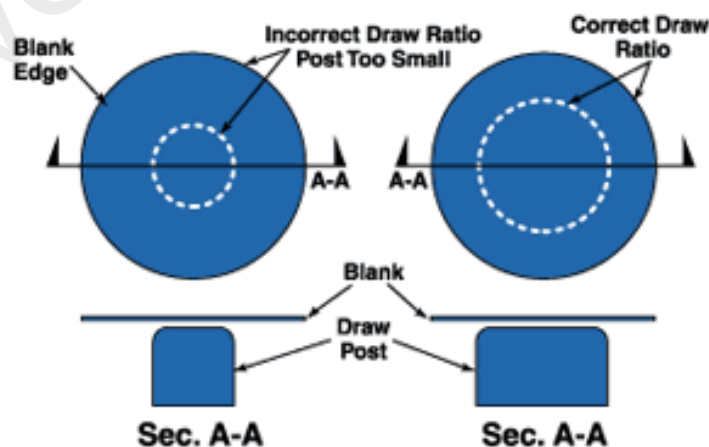
Figure 2.10: Draw ratio schematic diagram

The LDR is defined as the highest value of the ratio of the blank diameter to punch diameter which can be drawn out without failure. LDR is a close relationship with a diameter of the punch, lubrication, BHF, clearance between blank and punch. Anisotropy of the material of the blank will affect LDR as well.

Guo & Bleck (2016) stated that delayed cracking appeared in deep drawn specimens of high strength steel which endure strain-induced phase transformation. By raising the drawing ratio, which subsequently raised the maximum transformed martensitic fraction and residual stress in the drawn specimens, delayed cracking is facilitated as shown in Figure 2.11.
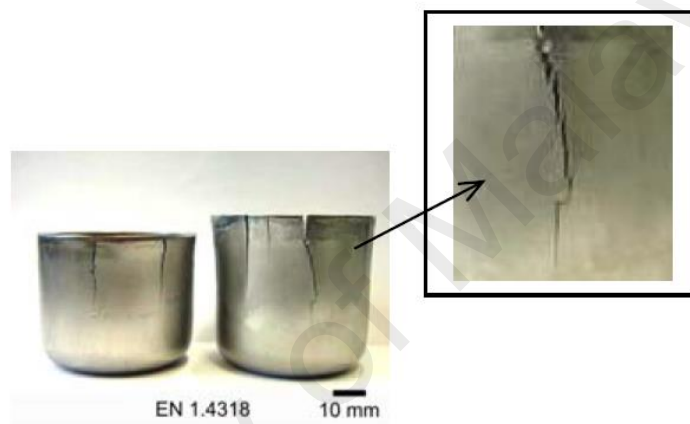
Figure 2.11: Delayed crack in high strength steel drawn cup (Guo & Bleck, 2016)

Papula et al. (2015) reported that the highest LDR will cause delayed crack in SUS301 deep drawn cup as shown in Figure 2.12. Berrahmoune et al. (2006) found that deep-drawn of 301 LN cups with the drawing ratio equal to 2.00 shows delayed cracking after 1 day of forming.

Figure 2.12: Stainless steel 301 deer drawn cut at drawing ratios 1.8, 1.9, 2.0 and 2.12 (Papula et al., 2015)

2.5   Previous Research on Eliminating Delayed Cracking

2.5.1   Annealing

Annealing is the process that heats metal or glass and allows it to cool slowly, in order to remove internal stresses and toughen it. Ragab & Orban (2000) stated that the residual stresses of the deep-drawn cup could be removed by annealing. The hydrogen content able to reduce by annealing thus increases the stability of austenite. The research done by Papula et al. (2014) shows that the hydrogen content of metastable austenitic stainless steel will reduce after the annealing at 400 °C. However due to annealing is costly and difficulties in maintaining the tolerance and surface finish, thus in most cases annealing process are not desired.

2.5.2   Ironing

Ironing is a very useful metal forming process when employed in combination with deep drawing to produce a uniform wall thickness cup with a greater height-to-diameter ratio. The clearance is less than the metal thickening on the flange side, the metal in the cup wall is squeezed. In the ironing process, a previously deep-drawn cup is drawn through an ironing ring with a moving ram to reduce the wall thickness. It means that quality can be promised. However, this ironing process required costly tools and advanced lubricants.

According to Ragab & Orban (2000), ironing can be used to reduce the residual stresses in deep drawn cups. Danckert (1995) proves that the ironing process causes a drastic change in the residual stress and causes a favorable distribution with regard to fatigue strength, stress corrosion resistance and stress cracking.

2.5.3   Elevated BHF

The concentration of the deformation-induced martensite is the highest along the cup edge, leading to an increase in the risk of the cracks. Reducing the degree of wall thickening along the cup edge with elevated BHF will lower the concentration of the martensite and the risk of crack.

El Sherbiny et al. (2014) stated that enhanced BHF able to decrease the sidewall thickness thus change the residual stress distributions of the drawn cups. In the previous study done by Tan et al. (2018), the cracks were successfully eliminated with an increase in BHF ranging from 3.6 to 3.9 times the minimum pressure required to suppress the wrinkle aided by nano-lubrication using a polished and uncoated die. However, nano-lubrication is costly and lower BHF is more desired instead of Higher BHF. This may due to higher BHF lead to a higher risk of material fracture, while the insufficient of BHF will cause the material wrinkled.

2.6   Coated Die

The coating is a covering that is applied to the surface of an object, usually referred to as the substrate. The purpose of applying the coating may be decorative, functional, or both. The coating itself may be an all-over coating, completely covering the substrate, or it may only cover parts of the substrate.

Die coating is widely used to enhance the tool life and its tribological performance. Abe, Ohmi, Mori, & Masuda (2014) found that deep draw-ability will improve if the coated die was used and VC-coated die is suitable for deep drawing of ultra-high-strength steel sheets. While Murakawa (1995) found that DLC film coated onto the die able to deep-draw aluminum sheets without any lubricant.

2.7   Titanium Nitride Coating

Thanks to its noble appearance, excellent adhesion to substrates, resistance to elevated temperatures, hard surfaces (2400HV) to reduce abrasive wear and a low coefficient of friction, TiN coating has been widely used for cutting tool and dies coating (Zhang & Zhu, 1993). A well-known use for TiN coating is for edge retention and corrosion resistance on machine tooling, such as drill bits and milling cutters, often improving their lifetime by a factor of three or more.

TiN is a golden yellow refractory compound of low density (5.22 g/cm 3) and a high melting point (2930 °C). There are two common methods in which TiN thin films are coated to the tooling include Chemical Vapor Deposition (CVD) and Physical Vapor Deposition (PVD).

In the CVD coating process, TiN coating is obtained from the chemical reaction between Titanium Tetrachloride, Nitrogen and Hydrogen. The chemical reaction takes place at a temperature typically between 850°C and 1100°C. PVD processes, on the other hand, operate at much lower temperatures between 400°C and 600°C. PVD coating process takes place in a vacuum chamber, the coating material such as Titanium is vaporized and the reactive Nitrogen gas is introduced and ionized. The vaporized titanium atoms then react with the ionized nitrogen to form the TiN compound that deposits on the substrate to form the coating.

Chapter 3 METHODOLOGY

3.1   Blanks

Laser-cut circular SUS304 blanks with 72mm diameter and 1.2 mm thickness were used in the deep drawing test. The hard cutting edge of the SUS304 blanks was polished using Grade 300 and Grade 400 sandpaper to remove the hard oxide layer and uneven edge which formed during the laser cut process. Figure 3.1 shows the circular SUS304 blanks, Table 3.1 and Table 3.2 show the chemical properties and mechanical properties.
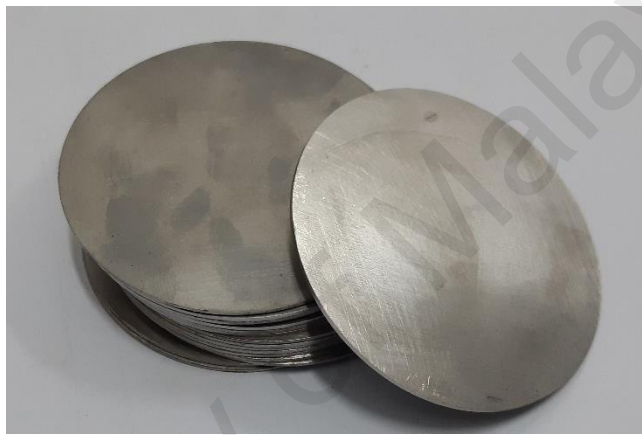
Figure 3.1: Circular SUS304 blanks

Table 3.1: Chemical properties of SUS304 blanks

Carbon	Silicon	Manganese	Phosphorus	Sulfur	Nickel	Chromium	Nitrogen
0.068	0.52	0.97	0.025	0.007	8.07	18.7	0.029

Table 3.2: Mechanical properties of SUS304 blanks

Tensile Strength	666 MPa
Yield strength	276 MPa
Elongation	54%
Hardness	86 HRB

3.2 Determine Limiting Drawing Ratio

As mentioned earlier, this research only deep drawn cup at its LDR will be investigated. because the delayed crack most likely will occur at LDR. The LDR is determined by the following formula:

$$LDR = \frac{Diameter_{Blank}}{Diameter_{Punch}}$$

The diameter of blanks and punch is 72mm and 34mm respectively. The LDR for the blank that uses in this research was 2.12, thus the draw ratio in this research was maintained at 2.12.

3.3 Experiment Setup

The experiment setup for the deep drawing is shown in Figure 3.2. The deep drawing was performed with a 25-ton motorized controlled shop press at a constant travel speed of approximately 1.1mm/s. A laser distance sensor (LVDT) and a 30-ton load cell were between the support plate and press. These devices were used to capture signals for the displacement of punch and forming load in the deep drawing process. Both signals are captured and recorded with a data logger with a sampling rate of 10 Hz.
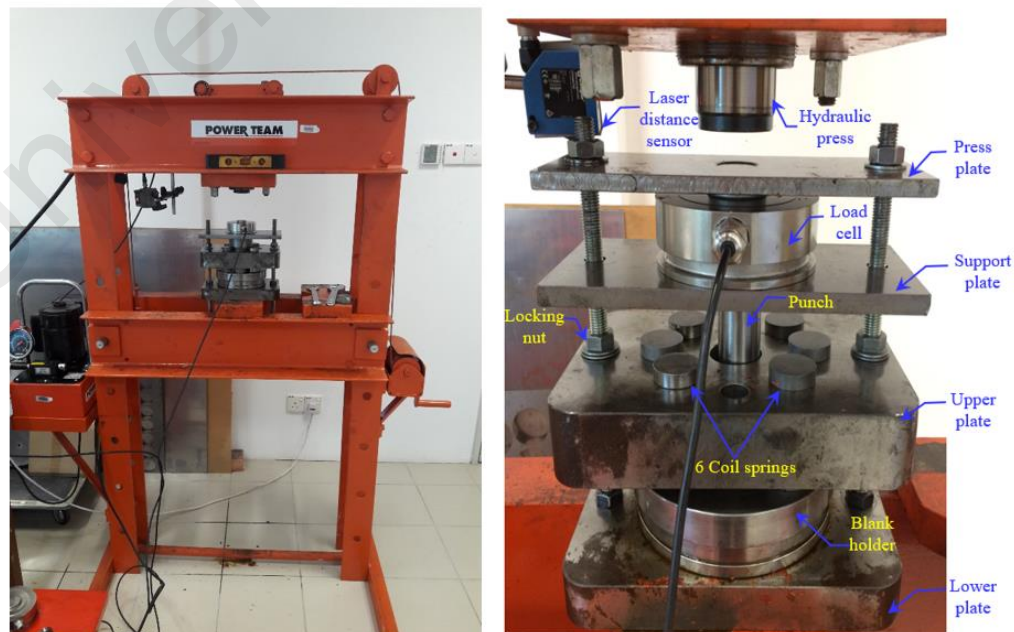
Figure 3.2: Experiment setup for the deep drawing test

3.3.1 Drawing Die

This experiment divided into two main parts including drawing test with the TiN coated die and deep drawing test with SKD-11 tool steel uncoated die. Both deep drawing tests were performed on the same setup and the same condition. Figure 3.3 shows the TiN coated die and SKD-11 tool steel uncoated die. The surface roughness of the TiN-coated die and SKD-11 tool steel uncoated die play an important role, thus it is necessary to measure it. The surface roughness of the TiN-coated die and SKD-11 tool steel uncoated die was measured by Mitutoyo SJ-210 surface roughness tester as shown in Figure 3.4. The surface roughness tester is tune to work under standard ISO1997. The direction of movement stylus tip of the roughness tester is shown in Figure 3.4, and the total travel length for the stylus tip is 12.5mm with a constant speed of 0.5mm/s.

Figure 3.3: TiN coated die (right) and SKD-11 tool steel uncoated die (left)
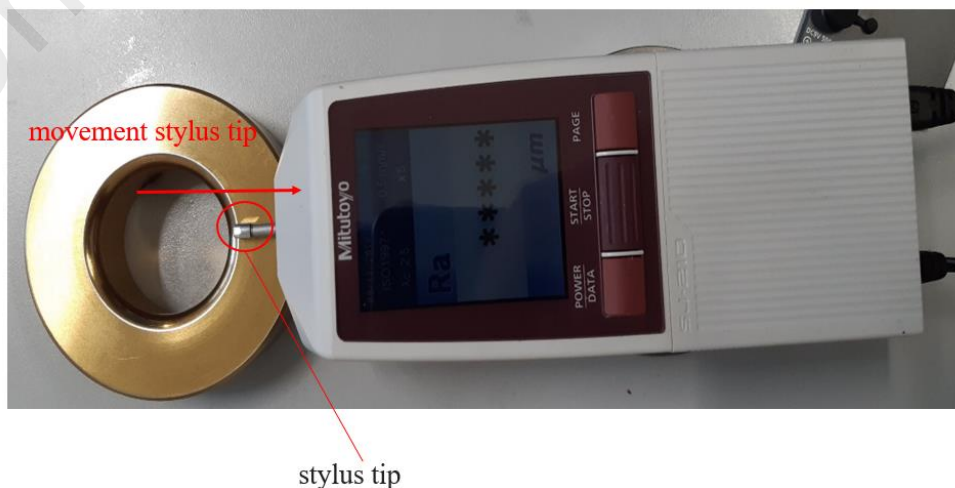
Figure 3.4: Surface roughness tester

The value of surface roughness for the SKD-11 tool steel uncoated die is measured after the polishing process with the aid of orbital sander polisher machine with 4000 rpm rotational speed. The polishing process starts with Grade 800 sandpaper follow by Grade 1000 sandpaper. Finally, a diamond paste that uses together with a compatible diamond lubricant is used for the final step of the polishing process. The specification of the diamond paste is shown in Table 3.3. For the TiN coated die, no polishing process is required.

Table 3.3: Specification of diamond paste

Product Code	3(W)45-MA
Application	Final finishing grades for most molds, dies, flat lapping and assorted production lapping
Micron size range	2-4
Approximate mesh size comparison	8000
Colour	Green
Diamond concentration	Standard medium strong
Type of diamond	Monocrystalline

From the measurement result (refer to Appendix A and Appendix B), the average surface roughness for TiN coated die and SKD-11 tool steel uncoated die is 0.382µm and 0.581µm respectively. It is shown that the TiN coated die has a smoother surface than the SKD-11 tool steel uncoated die as its average surface roughness is lower. Figure 3.5 and Figure 3.6 show the surface roughness evaluation profile for both TiN coated die and SKD-11 tool steel uncoated die respectively.
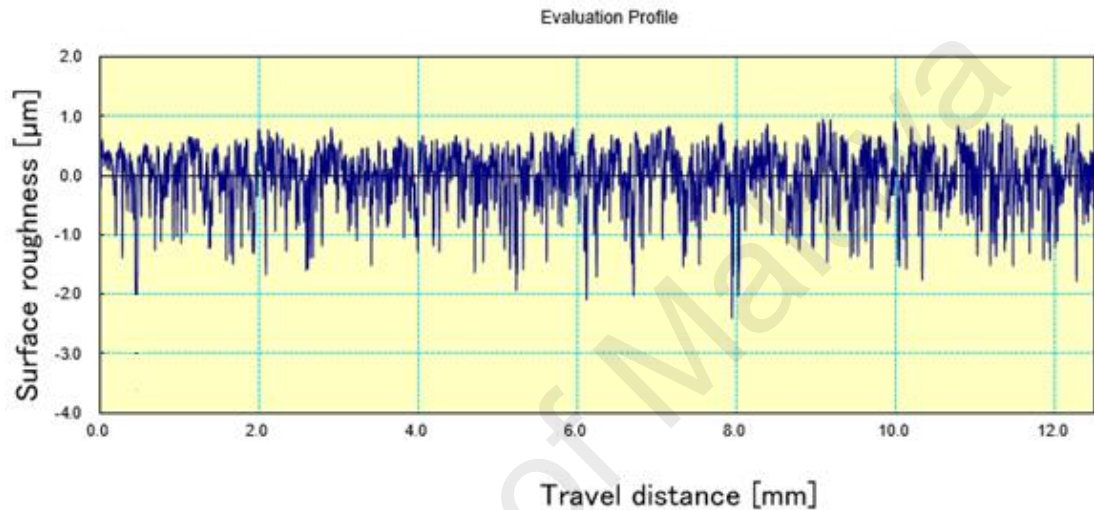
Figure 3.5: Surface roughness profile of TiN coated die
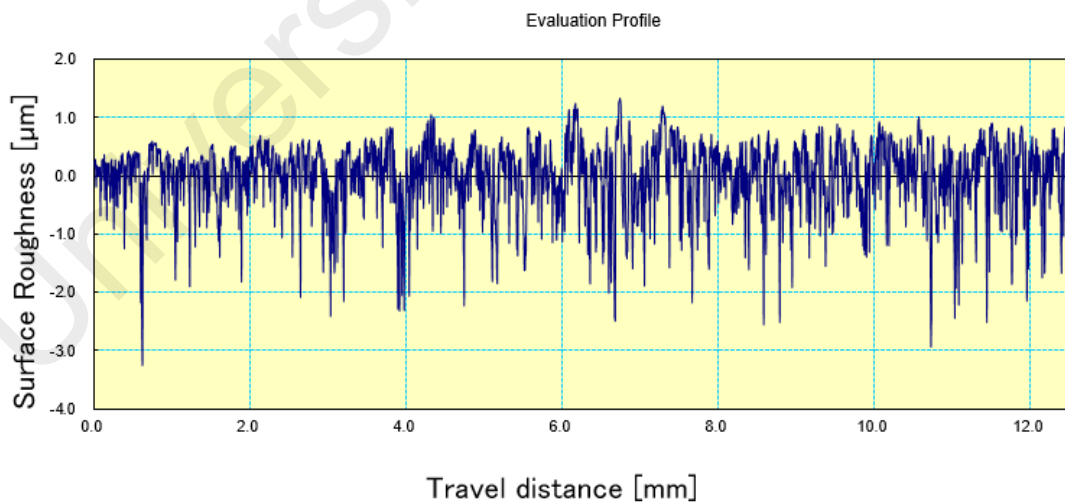
Figure 3.6: Surface roughness profile of finely polished SKD-11 tool steel uncoated die

3.3.2   Setting of BHF

It was important to define the BHF range that able to form the cup successfully. The deep drawing test starts with initial BHF of 8kN, then the deep drawing test BHF repeat by further decrease with a step size of 1kN until the wrinkle appears along the sidewall of the cup. When wrinkle appears along the sidewall of the cup it indicates the lower limits of BHF. The deep drawing test was repeated by further increase with a step size of 1kN until the formation of fracture at the cup bottom. When a fracture occurs, it indicates the upper limits of BHF. A total of two deep-drawn cups will be formed for each value of BHF. If the first two deep drawing test results were conflicting, the third deep drawing test will be performed.

When setting the target BHF the LVDT sensor, punch, press plate, support and 30-ton load cell plate were being removed. A cylindrical block was placed between the upper plate and the support plate, while a 10-ton load cell was used to measure the target BHF as shown in Figure 3.7.

Figure 3.7: Setup for generating and measure the target BHF

The Commercial JSM coil springs located inside the upper plate was then compressed by a hydraulic press to target BHF value. All coils had a spring constant of 0.785 kN/mm with a maximum deflection of 8 mm. In order to obtain a balanced holding force toward the blank, the coils were arranged symmetrically. The tightening locking nuts above the upper plate will prevent coil return by without increasing or decreasing the target BHF value.

3.3.3 Deep Drawing Test

Before the deep drawing test, the punch, press plate, support plate and the 10-ton load cell was replaced by a 30-ton load cell. The LVDT sensor was put back to its original position as well.

The circular SUS304 blank is accurately positioned to the center of the die with the aided of the digital caliper. The punch diameter of punch and both SKD-11 tool steel uncoated die and TiN coated die were fixed at 34mm and 37.4mm respectively. Both punch and die have a corner radius of 5mm. The clearance between punch and die was set larger than the thickness of SUS304 blank to allow the sidewall to freely thicken due to circumferential compression during the deep drawing process.

A commercial lubricant will be applied on the die surface, the die corner and blank holder surfaces. The lubricant able to prevent minimize surface damage on the die, prevent excessive friction between blank and blank holder. The punch and blank surface were kept dry. The die surface and blank holder surface were inspected for wear at the end of each test and the surface was polished with Grade 800 sandpaper, Grade 1000 sandpaper and diamond paste before the next deep drawing test. Noted that the polish process was not applied to the TiN coated die surface. Figure 3.8 shows the detail conditions for the deep drawing test.
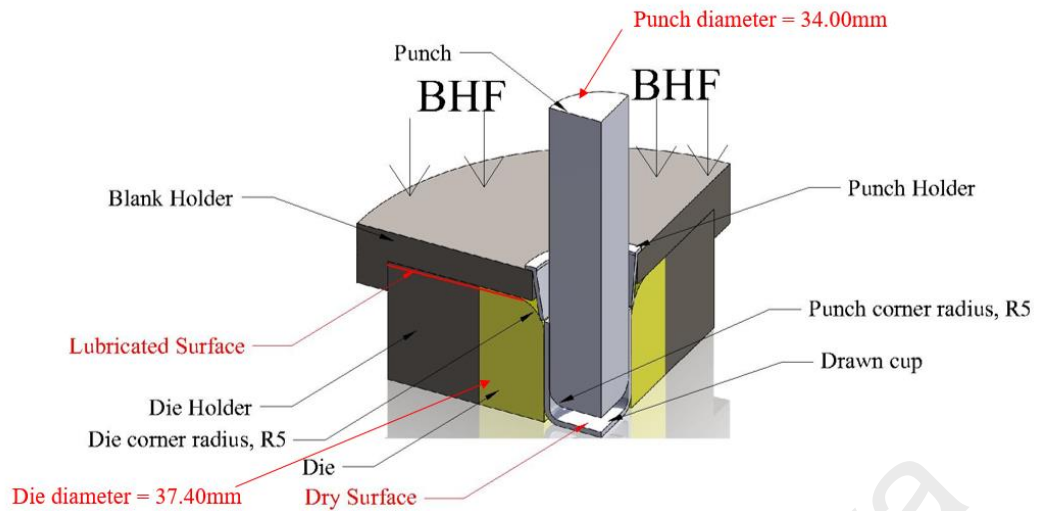
Figure 3.8: Detail conditions for the deep drawing test

3.4 Ring Slitting Method

The residual stresses along the sidewall of deep-drawn cups were estimated using a ring slitting method that bases on the concept of residual stress relaxation. Deep drawn cups were sectioned with electrical discharge machining (EDM) into rings. The slit rings obtained for cup heights of 30%, 60%, 80%, and 100% from the bottom of the deep-drawn cup. The rings are then slit in the longitudinal direction with EDM to obtain an opening gap. Figure 3.9 shows the schematic diagram for the ring slitting method.

Figure 3.9: Ring slitting method

The ring-opening distance, the inner diameter of the ring before slitting and the sidewall thickness of the ring were measured and recorded. The residual stresses were then computed using the formula:

$$\sigma = E \bullet t \left(\frac{1}{D_o} - \frac{1}{D_o + \dfrac{d-s}{\pi}} \right)$$

Where:

E = modulus of elasticity (200 GPa)

T = ring wall thickness

D_o = inner ring diameter before slitting

d = ring-opening gap

s = EDM wire diameter (0.2mm)

3.5 Peak Point and Valley Point Measurement

Since the valley points have higher chances for the delayed cracks. Thus, it is necessary to take focus on the change in wall thickness of valley point and peak point, and cup height measured from cup bottom to valley point and peak point respectively. The thickness and height will measure by micrometers screw gauge and height gauge respectively as shown in Figure 3.10.

Figure 3.10: Micrometres screw gauge and height gauge

Besides that, the change in wall thickness as the valley will be calculated and discuss as well. The change in wall thickness in valley point will be calculated by the formula:

$$\% change = \frac{(measure\ thickness - initial\ thickness)}{initial\ thickness} x 100\%$$

Chapter 4 RESULTS AND DISCUSSION

4.1   Drawing Results for SKD-11 Tool Steel Uncoated Die

The successful cup forming BHF range for polished SKD-11 tool steel uncoated die was 6kN to 15kN. While the lower and upper limit BHF were 5kN and 16kN respectively as wrinkle and fracture appear on these two BHF values. Within its successful cup forming BHF range, the only crack free BHF was 12kN. Table 4.1 and APPENDIX A summarize the drawing results for the SKD-11 tool steel uncoated die. The forming loads for different BHF using the SKD-11 tool steel uncoated die were presented in Figure 4.1.

Table 4.1: Drawing results for SKD-11 tool steel uncoated die

BHF (kN)	Delayed Crack	Remark
6	-	Lower limits of BHF (Wrinkle appear)
7	YES	
8	YES	
9	YES	
10	YES	
11	YES	
12	NO	
13	YES	
14	YES	
15	YES	
16	-	Upper Limit of BHF (Fracture at the cup bottom)
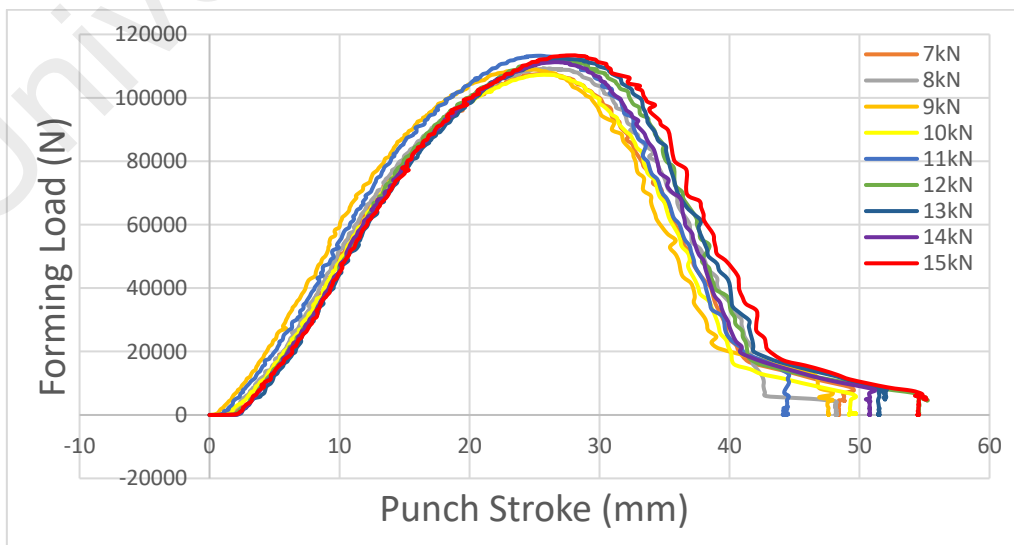
Figure 4.1: Forming loads for different BHF using SKD-11 tool steel uncoated die

The number of cracks and duration measures in hours for the first crack to appear with different BHF was summarized in Table 4.2 and presented in Figure 4.2. The duration for the first crack to appear increase with the increase of BHF. The duration decreased significantly from 14 hours at BHF of 13kN to 4 hours at BHF of 14kN and 15kN, this may due to the lubricant performance was exceeded its limit.

Table 4.2: Number and time taken for the appearance of the first crack for different BHF

BHF (kN)	No. of Crack	Duration for First Crack (hours)
5	1	2.5
6	1	5
7	1	8
8	2	9.5
9	1	9
10	1	11
11	1	13
12	0	0
13	3	14
14	1	4
15	1	4
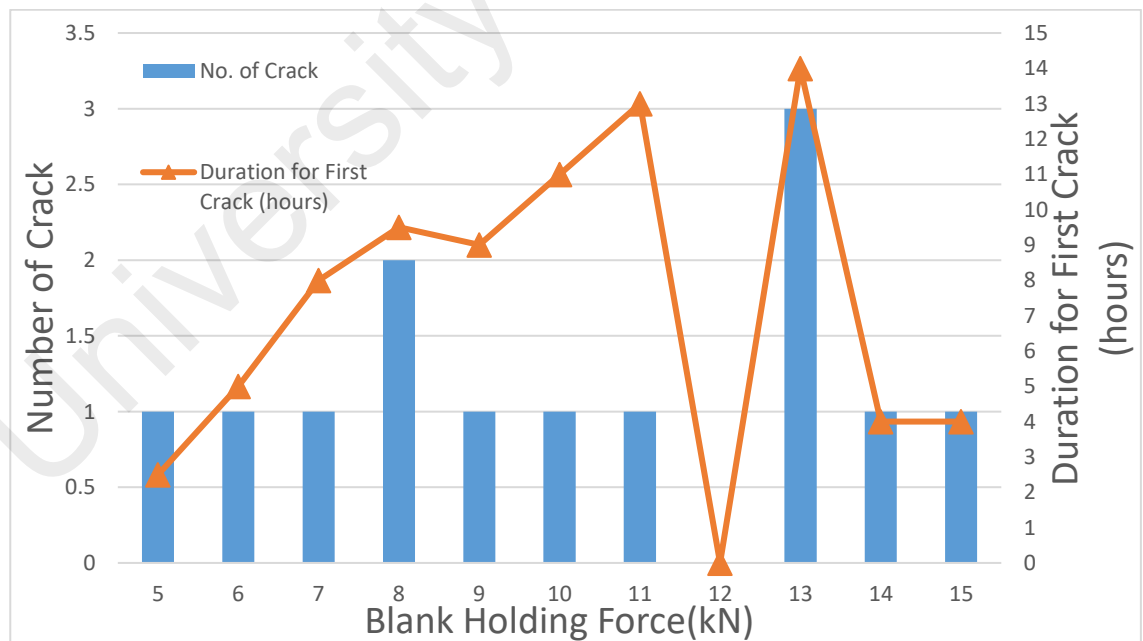
Figure 4.2: Comparison of number and time taken for the first appearance of the delayed crack

From the deep drawing test results, the deep-drawn cup form by the SKD-11 tool steel uncoated die was suffering in the delayed crack. Since the previous research shown that the coated die has an advantage against uncoated to improve the deep draw-ability. Thus, it is interesting to study how the performance of coated die on suppresses the delayed crack. The deep drawing test was repeated by using a TiN coated die.

4.2   Drawing Results for TiN Coated Die

The successful cup forming BHF range for TiN coated die was 5kN to 10kN. While the lower and upper limit BHF were 4kN and 11kN respectively as wrinkle and fracture appear on these two BHF values. Within its successful cup forming BHF range, no delayed crack was found. Table 4.3 and APPENDIX B summarize the drawing results for TiN coated die. The forming loads for different BHF using TiN coated die were presented in Figure 4.3.

Table 4.3: Drawing results for TiN coated die

BHF (kN)	Delayed Crack	Remark
4	-	Lower limits of BHF (Wrinkle appear)
5	NO	
6	NO	
7	NO	
8	NO	
9	NO	
10	NO	
11	-	Upper Limit of BHF (Fracture at the cup bottom)
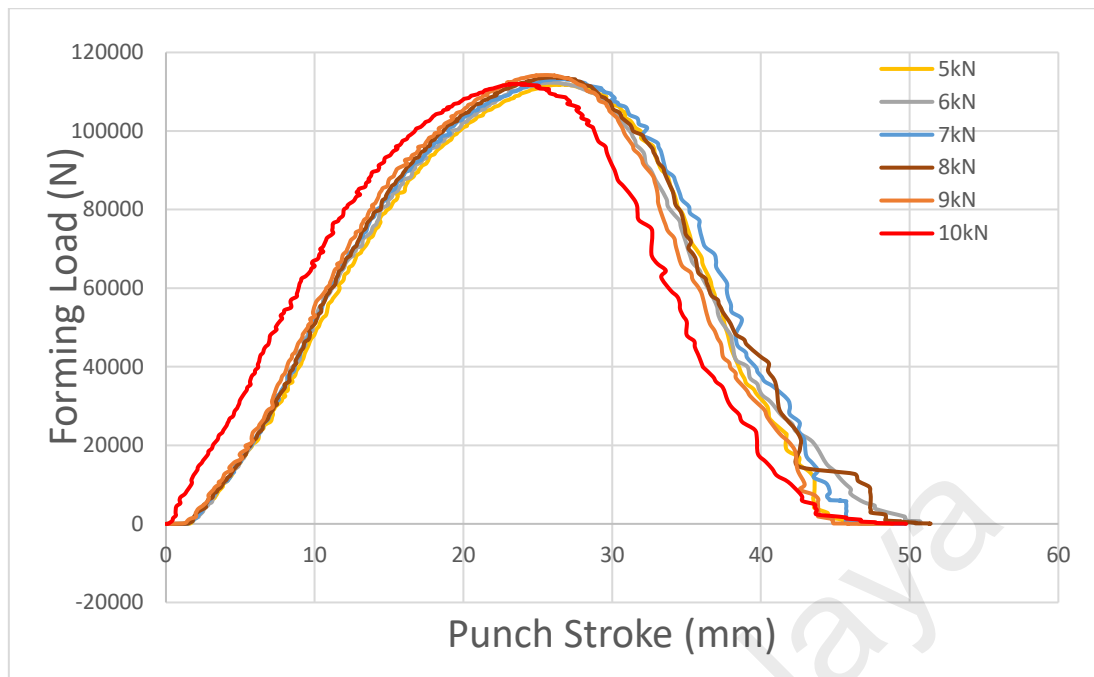
Figure 4.3: Forming loads for different BHF using TiN coated die

The lower and the upper BHF limits between the cups formed with the uncoated die and the ones formed with the coated die. For example, 7kN to 15kN for SKD-11 tools steel uncoated die lowers to 5kN to 10kN for TiN coated die due to the improved surface roughness of the coated die. However, the tribological performance of the coated surface is lower than the one for the uncoated surface under the elevated BHF, resulting in a smaller BHF range.

In the previous study by Tan et al. (2018), the cracks were successfully eliminated with uncoated die aided with nano-lubricant under BHF of 8kN to 32kN. The widest crack-free BHF range determined experimentally was 2% of SiO_2 nano-particle under BHF range 29kN to 31kN. Although the BHF lower and upper limit for uncoated die aided by nano-lubricant is very much wider than the ones for the coated die, the delayed-crack-free BHF range is smaller than the coated die. Although the nano-lubricant has increased the forming limit of the cup, there is no significant increase in the delayed crack free BHF range.

In the previous study by Thye (2017), the delayed crack was successfully eliminated with TiN coated die aided with 2% of SiO_2 nano-particle. Although the BHF for the upper forming limit of the successfully drawn cups was increased by the addition of the nano-lubricant to the TiN coated die, for example, 14kN to 19kN (there is a fracture founded at 16kN). However, the delayed-crack-free BHF range significantly reduced, the delayed crack free cups were obtained at BHF equal to 15kN only. Thus, in this research, the nano-lubricant was replaced by the commercial lubricant.

The relationship between the BHF and peak forming load for both SKD-11 tools steel uncoated die and TiN coated die is shown in Figure 4.4. Generally, the peak forming load increase with the increase of the BHF. Under common BHFs value (7kN, 8kN, 9kN and 10kN) for both coated and uncoated die, the peak forming load for TiN coated is must lower than SKD-11 tools steel uncoated die. The lower peak forming loads indicate a better lubricant effect of TiN coated die under the same BHF values.
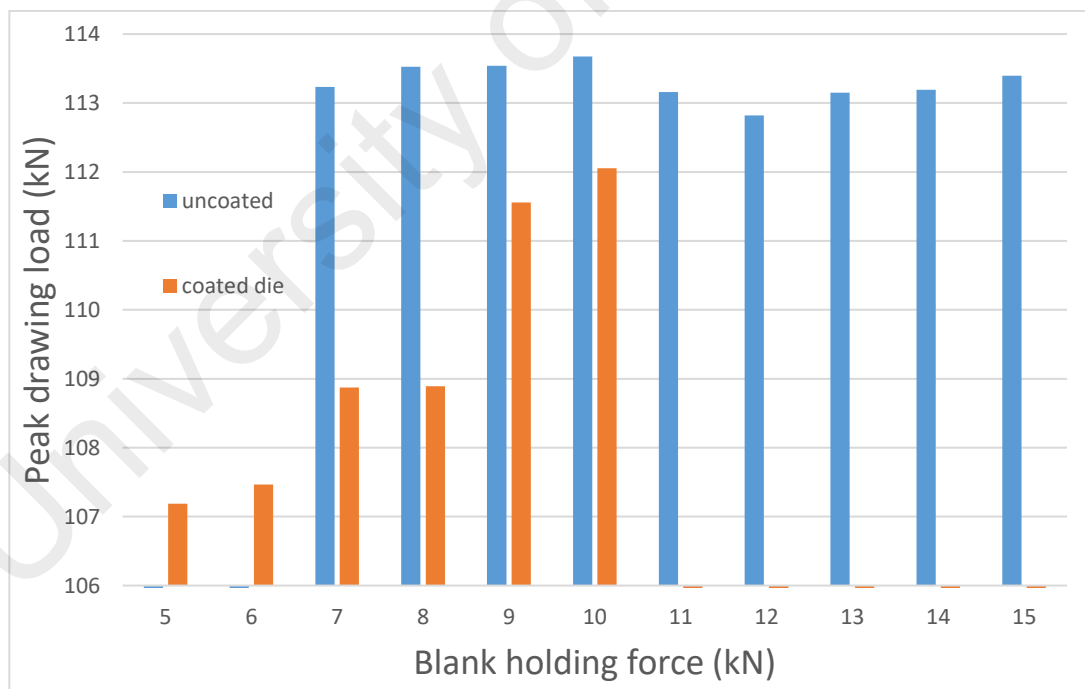
Figure 4.4: Relationship between the BHF and peak forming load for both SKD-11 tools steel uncoated die and TiN coated die

4.3 Peak Point and Valley Point Measurement Results

Table 4.4 and Table 4.5 shows the peak point and valley point measurement results for SKD-11 tool steel uncoated die and TiN coated die. APPENDIX C and APPENDIX D shown the position of the peak point and valley point for SKD-11 tool steel uncoated die and TiN coated die. Tan & Aslian (2019) stated that the valley points have higher chances for the delayed cracks, this statement agrees by the deep drawing test result. Refer to Table 4.4; it can be found that the delayed crack only occurs in the valley point of the deep-drawn cup.

Table 4.4: Peak point and valley point measurement results for SKD-11 tool steel uncoated die

BHF = 7 kN					
Valley Point			Peak Point		
Position	Thickness(mm)	Height(mm)	Position	Thickness(mm)	Height(mm)
V1*	1.762	31.10	P1	1.428	33.06
V2	1.608	31.92	P2	1.422	34.06
V3	1.656	32.28	P3	1.424	35.28
V4	1.606	33.44	P4	1.350	34.80
Average	**1.658**	**32.19**	**Average**	**1.406**	**34.30**
BHF = 8 kN					
Valley Point			Peak Point		
Position	Thickness(mm)	Height(mm)	Position	Thickness(mm)	Height(mm)
V1*	1.809	31.41	P1	1.502	33.76
V2	1.696	32.16	P2	1.521	34.07
V3*	1.831	31.78	P3	1.515	33.88
V4	1.625	32.19	P4	1.514	33.42
Average	**1.740**	**31.89**	**Average**	**1.513**	**33.78**
BHF = 9 kN					
Valley Point			Peak Point		
Position	Thickness(mm)	Height(mm)	Position	Thickness(mm)	Height(mm)
V1*	1.627	32.08	P1	1.478	34.84
V2	1.624	32.50	P2	1.436	34.38
V3	1.649	32.54	P3	1.429	33.10
V4	1.625	32.50	P4	1.428	34.68
Average	**1.631**	**32.41**	**Average**	**1.442**	**34.25**
BHF = 10 kN					
Valley Point			Peak Point		
Position	Thickness(mm)	Height(mm)	Position	Thickness(mm)	Height(mm)
V1*	1.742	31.34	P1	1.371	34.76
V2	1.543	33.50	P2	1.403	35.00
V3	1.552	32.86	P3	1.456	34.14
V4	1.570	31.82	P4	1.419	33.34
Average	**1.601**	**32.38**	**Average**	**1.412**	**34.31**
BHF = 11 kN					
Valley Point			Peak Point		
Position	Thickness(mm)	Height(mm)	Position	Thickness(mm)	Height(mm)
V1*	1.600	32.10	P1	1.440	34.26

Position	Thickness(mm)	Height(mm)	Position	Thickness(mm)	Height(mm)
V2	1.654	32.26	P2	1.387	34.62
V3	1.576	33.12	P3	1.406	34.20
V4	1.679	33.44	P4	1.408	34.44
Average	**1.627**	**32.73**	**Average**	**1.410**	**34.38**
BHF = 12 kN					
Valley Point			Peak Point		
Position	Thickness(mm)	Height(mm)	Position	Thickness(mm)	Height(mm)
V1	1.649	33.64	P1	1.361	34.66
V2	1.534	33.64	P2	1.354	35.00
V3	1.539	33.69	P3	1.402	34.52
V4	1.424	33.62	P4	1.404	34.56
Average	**1.537**	**33.65**	**Average**	**1.380**	**34.69**
BHF = 13 kN					
Valley Point			Peak Point		
Position	Thickness(mm)	Height(mm)	Position	Thickness(mm)	Height(mm)
V1*	1.546	32.54	P1	1.445	34.36
V2	1.571	32.42	P2	1.489	34.42
V3*	1.577	32.43	P3	1.489	34.44
V4*	1.859	32.60	P4	1.342	34.12
Average	**1.638**	**32.49**	**Average**	**1.441**	**34.34**
BHF = 14 kN					
Valley Point			Peak Point		
Position	Thickness(mm)	Height(mm)	Position	Thickness(mm)	Height(mm)
V1*	1.843	31.84	P1	1.398	34.48
V2	1.632	32.42	P2	1.386	34.28
V3	1.688	32.34	P3	1.347	34.12
V4	1.530	32.84	P4	1.379	34.30
Average	**1.673**	**32.47**	**Average**	**1.378**	**34.30**
BHF = 15 kN					
Valley Point			Peak Point		
Position	Thickness(mm)	Height(mm)	Position	Thickness(mm)	Height(mm)
V1*	1.841	31.42	P1	1.380	34.22
V2	1.600	32.42	P2	1.410	34.72
V3	1.631	32.34	P3	1.419	34.05
V4	1.573	32.84	P4	1.378	34.16
Average	**1.661**	**32.26**	**Average**	**1.397**	**34.29**

Note:
* indicate the delayed crack

Table 4.5: Peak point and valley point measurement results for TiN coated die

| BHF = 5 kN |
| Valley Point | | | Peak Point | | |
Position	Thickness(mm)	Height(mm)	Position	Thickness(mm)	Height(mm)
V1	1.577	33.54	P1	1.495	35.62
V2	1.583	33.52	P2	1.365	35.40
V3	1.585	33.48	P3	1.455	33.25
V4	1.581	33.30	P4	1.421	33.98
Average	1.582	33.46	Average	1.434	34.56
BHF = 6 kN					
Valley Point			Peak Point		
Position	Thickness(mm)	Height(mm)	Position	Thickness(mm)	Height(mm)
V1	1.561	33.62	P1	1.408	35.22
V2	1.565	33.60	P2	1.418	34.70
V3	1.578	33.80	P3	1.417	34.87
V4	1.592	33.60	P4	1.413	35.43
Average	1.574	33.66	Average	1.414	35.06
BHF = 7 kN					
Valley Point			Peak Point		
Position	Thickness(mm)	Height(mm)	Position	Thickness(mm)	Height(mm)
V1	1.550	33.77	P1	1.390	35.38
V2	1.544	33.60	P2	1.435	35.86
V3	1.527	33.70	P3	1.406	34.52
V4	1.542	33.72	P4	1.405	34.19
Average	1.546	33.70	Average	1.409	34.99
BHF = 8 kN					
Valley Point			Peak Point		
Position	Thickness(mm)	Height(mm)	Position	Thickness(mm)	Height(mm)
V1	1.484	33.96	P1	1.352	35.16
V2	1.476	34.55	P2	1.368	35.30
V3	1.501	33.89	P3	1.382	35.21
V4	1.515	33.91	P4	1.439	35.37
Average	1.494	34.08	Average	1.385	35.26
BHF = 9 kN					
Valley Point			Peak Point		
Position	Thickness(mm)	Height(mm)	Position	Thickness(mm)	Height(mm)
V1	1.586	33.18	P1	1.411	34.42
V2	1.595	33.19	P2	1.404	34.44
V3	1.592	33.35	P3	1.374	35.39
V4	1.594	33.69	P4	1.409	35.35
Average	1.592	33.35	Average	1.400	34.90
BHF = 10 kN					
Valley Point			Peak Point		
Position	Thickness(mm)	Height(mm)	Position	Thickness(mm)	Height(mm)
V1	1.574	33.32	P1	1.404	35.10
V2	1.587	33.35	P2	1.419	35.14
V3	1.595	33.38	P3	1.412	34.96
V4	1.586	33.33	P4	1.402	35.12
Average	1.586	33.35	Average	1.409	35.08

Figure 4.5 illustrates the average peak and valley point heights along the cup edge measured from the bottom for different BHF.
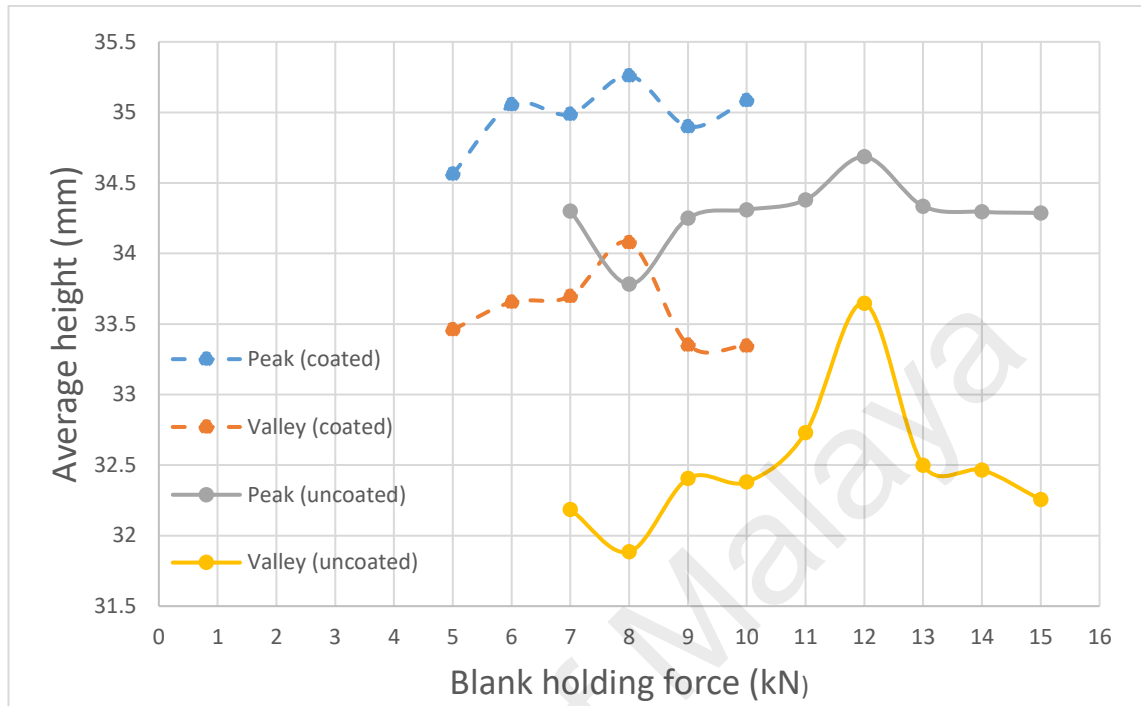
Figure 4.5: Average peak and valley point heights

For deep drawn cup form by TiN coated die, the highest and lowest average height for valley point was 34.08mm and 33.35mm with BHF value 8kN and 9-10kN respectively. The highest and lowest average height for peak point was 35.26mm and 34.56mm with BHF value 8kN and 5kN respectively.

For deep drawn cup form by SKD-11 tool steel uncoated die, the highest and lowest average height for valley point was 33.65mm and 31.89mm with BHF value 12kN and 8kN respectively. The highest and lowest average height for peak point was 34.69mm and 33.78mm with BHF value 12kN and 8kN respectively. For the crack-free BHF value 12kN, it has a greater average height for both peak and valley point, this indicates that the cup is elongated more compare to other cups formed by SKD-11 tool steel die.

Deep drawn cup form by TiN coated die have the smaller differences between the highest and lowest average height for both valley point and peak point compare to the deep drawn cup form by SKD-11 tool steel uncoated die. The smaller the different shows that the smoother surface of the TiN coated die surface provides a lower frictional force and facilitated the flow of material into the hole gravity of die. Both forming results show that the peak point was higher than the valley point. In the common BHF for both die which from 7kN to 10kN, it can be found that the average height for both valley point and peak point of the deep-drawn cup formed by TiN coated die is generally higher than the average height of deep drawn cup formed by SKD-11 tool steel uncoated die.

Table 4.6 and Table 4.7 shows the average change in wall thickness of peak point and valley point for both deep drawn cup formed by TiN coated die and SKD-11 tool steel uncoated die.

Table 4.6: Average change in wall thickness of peak point and valley point for deep drawn cup formed by SKD-11 tool steel uncoated die

BHF (kN)	The average change in wall thickness of peak point (%)	The average change in wall thickness of valley point (%)
7	17.17	38.17
8	26.08	45.02
9	20.23	35.94
10	17.69	33.48
11	17.52	35.60
12	15.02	28.04
13	20.10	36.52
14	14.80	39.44
15	16.40	38.44

Table 4.7: Average change in wall thickness of peak point and valley point for deep drawn cup formed by TiN coated die

BHF (kN)	The average change in wall thickness of peak point (%)	The average change in wall thickness of valley point (%)
5	19.50	31.79
6	17.83	31.17
7	17.42	28.81
8	15.44	24.50
9	16.63	32.65
10	17.44	32.13

Figure 4.6 illustrates the average change in wall thickness of both measured peak and valley point thickness along the cup edge compare to initial blank thickness under different BHF.
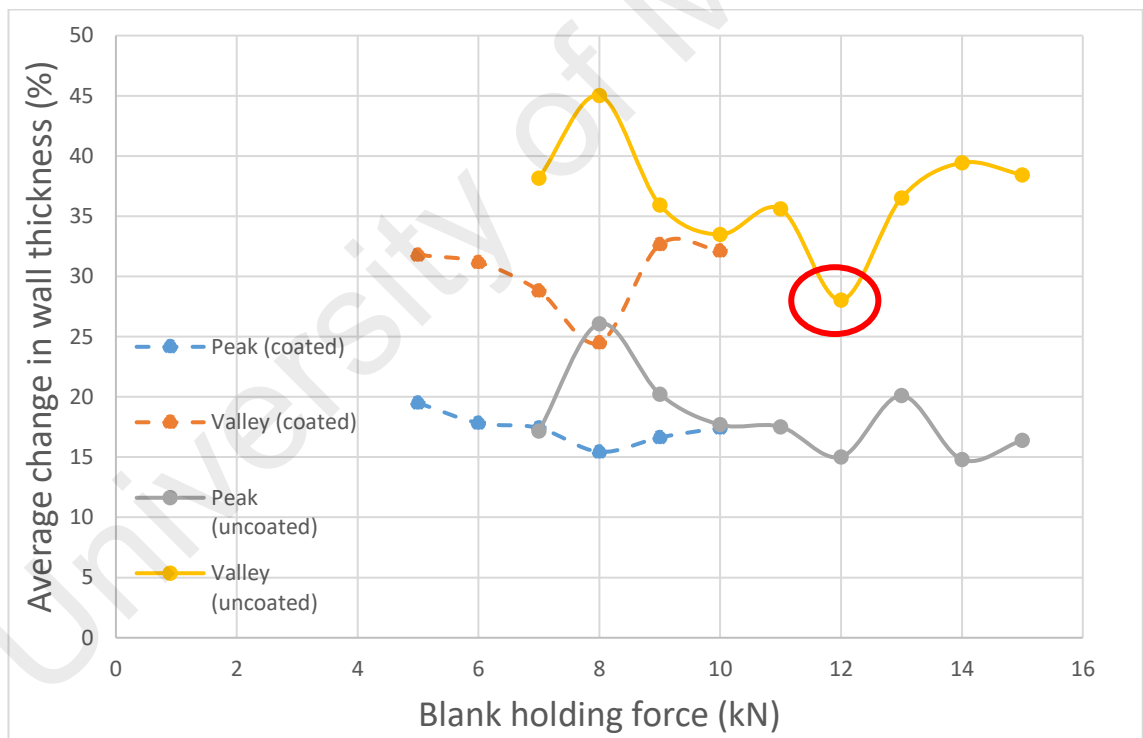

Figure 4.6: Average change in wall thickness for peak and valley point under different BHF

For deep drawn cup form by TiN coated die, the highest and lowest average change in wall thickness for valley point was 32.65% and 24.50% with BHF value 9kN and 8kN respectively. The highest and lowest average change in wall thickness for peak point was 19.5% and 15.44% with BHF value 5kN and 8kN respectively.

For deep drawn cup form by SKD-11 tool steel uncoated die, the highest and lowest average thickness for valley point was 45.02% and 28.04% with BHF value 8kN and 12kN respectively. The highest and lowest average change in wall thickness for peak point was 26.08% and 14.80% with BHF value 8kN and 14kN respectively.

Both forming results show that the valley point was thicker (greater positive value of change in wall thickness) than the peak point. It can be found that in the common BHF for both dies which from 7kN to 10kN, the average change in wall thickness for both valley point and peak point of the deep-drawn cup formed by TiN coated die is lower than the deep-drawn cup formed by SKD-11 tool steel uncoated die. This indicated that the lower amount of wall thickening.

From the deep drawing test results, it can claim that the delayed crack occurs only at the valley point of the deep-drawn cup. The parameter such as height and thickness of valley point will play an important role in suppressing the delayed crack. Generally, the deep-drawn cup formed by SKD-11 tools steel uncoated die has a higher amount of wall thickening in valley point. The higher amount of wall thickening in valley point lead to the higher risks for delayed crack. The only crack free cup among the cup formed by uncoated die with a BHF value of 12kN (with the circular marker). At this value of BHF, the deep-drawn cup has a lower value of change in wall thickness (28.04%) in valley point (low thickness), thus it was free from the delayed crack. This might due to the small thickness able to lower down the concentration of the deformation-induced martensite and change the residual stress distributions of the drawn cups thus reduce the risk of delayed crack.

The higher amount of wall thickening in valley point have a higher risk for delayed crack. This statement can be seen more clearly when comparing the valley point thickness under common BHF value (7kN, 8kN, 9kN and 10kN) for both coated and uncoated die. Figure 4.7 shows the comparison for the valley point thickness under common BHF value for both coated and uncoated die. The valley point position with red circle marking indicates the delayed crack, it can be found that the thicker valley point has a higher risk for delayed crack. Due to reaching the upper limit of the BHF value 10kN for coated die, the performance of lowering the degree of wall thickening effect decreased, thus some of the valley points may have thicker valley point. However, due to the small amount of wall thickening, the cup was free from the delayed crack.

Figure 4.7: Comparison for the valley point thickness under common BHF value

The relationship between the average cup height and the average change in wall thickness in the peak and the valley points for cups formed with the uncoated die under elevated BHF is shown in Figure 4.8. Overall, the amount of wall thickening in the valley point decreases with increasing valley point height for an increase in BHF up to 12kN. However, it shows a reverse trend for BHF greater than 12kN. Therefore, the delayed cracks were successfully prevented at the BHF value of 12kN due to the less

amount of deformation-induced martensite resulting from the lower amount of wall thickening.

The amount of wall thickening in valley points are higher than that of the peak points under all BHF values. Therefore, the chances for delayed cracks to form in the valley points are higher than the peak points. Despite having the same trend with the valley points, the amount of wall thickening in the peak points and the peak heights are less sensitive to the increase in BHF.

Figure 4.8: Relationship between BHF, average cup height and average change in wall thickness for deep drawn cup formed by SKD-11 tool steel uncoated die

The relationship between the average cup height and the average change in wall thickness in the peak and the valley points for cups formed with the TiN coated die under elevated BHF is shown in Figure 4.9. Overall, the trend is similar to the ones obtained with the uncoated die. The amount of wall thickening decreases with increasing height, particularly in valley points for an increase in BHF up to 8kN. The reverse trend is observed for BHF greater 8kN. However, the amount of change in both

values is less significant than the ones for the uncoated die under the elevated BHF as all cups formed within this BHF range are free from the delayed crack.
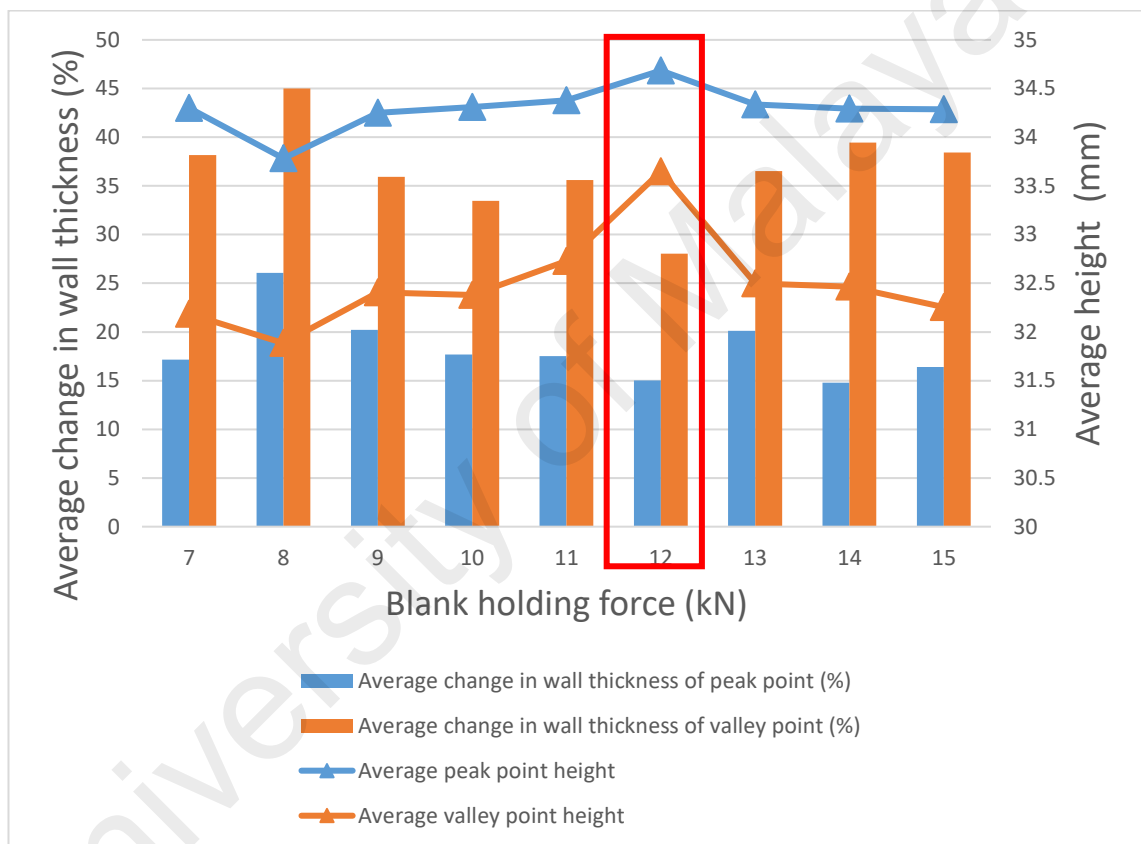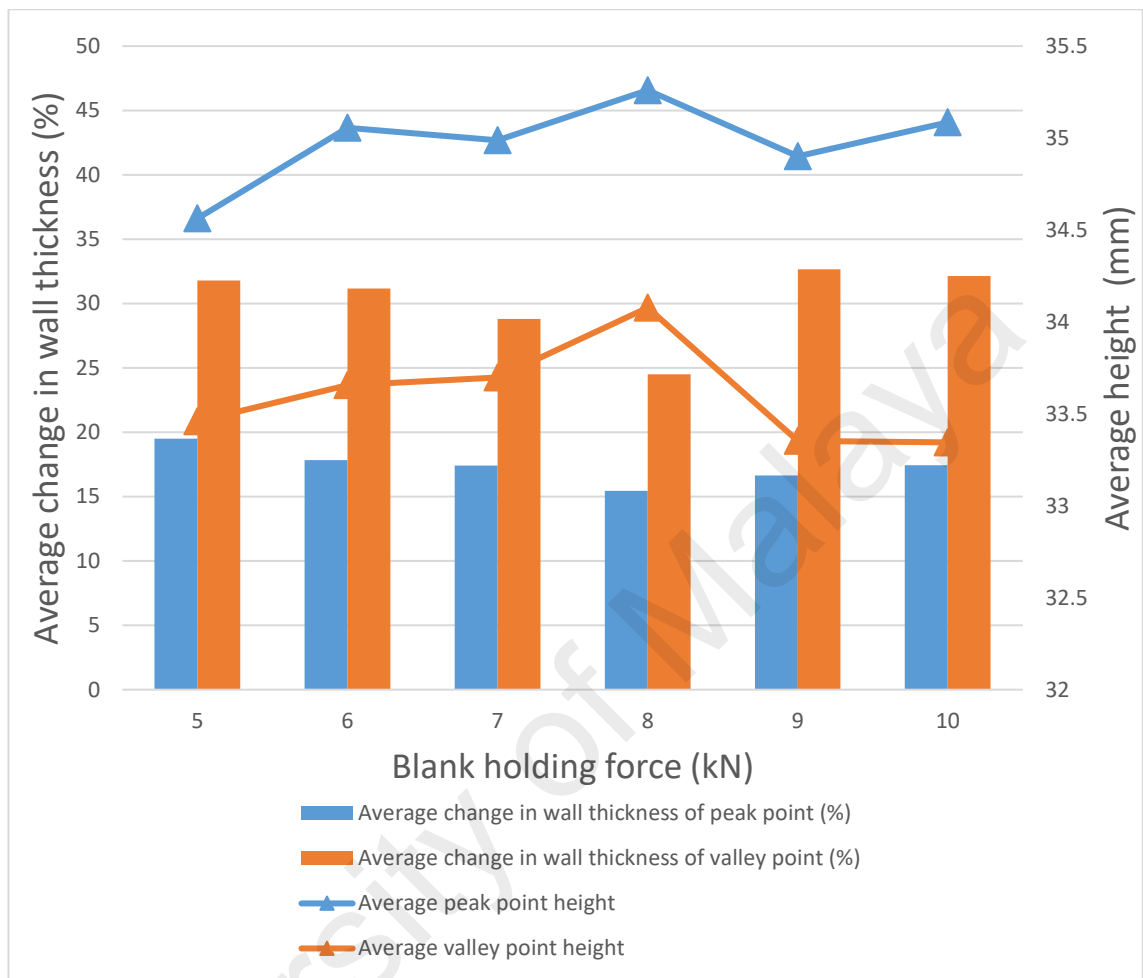

Figure 4.9: Relationship between BHF, average cup height and average change in wall thickness for deep drawn cup formed by TiN coated die

In order to clarify the performance of TiN coated die on lowering the amount of wall thickening. Thus, the change in wall thickness along circumference direction for both the cup by both coated and uncoated die was taken into account. This measurement could show the distribution of the material in the valley zone more clearly. This measurement will take with an increment of 1mm starting from position V1 as shown in Figure 4.10. The measurement result was presented in Figure 4.11.

Figure 4.10: Measurement of thickness distribution along the circumference direction
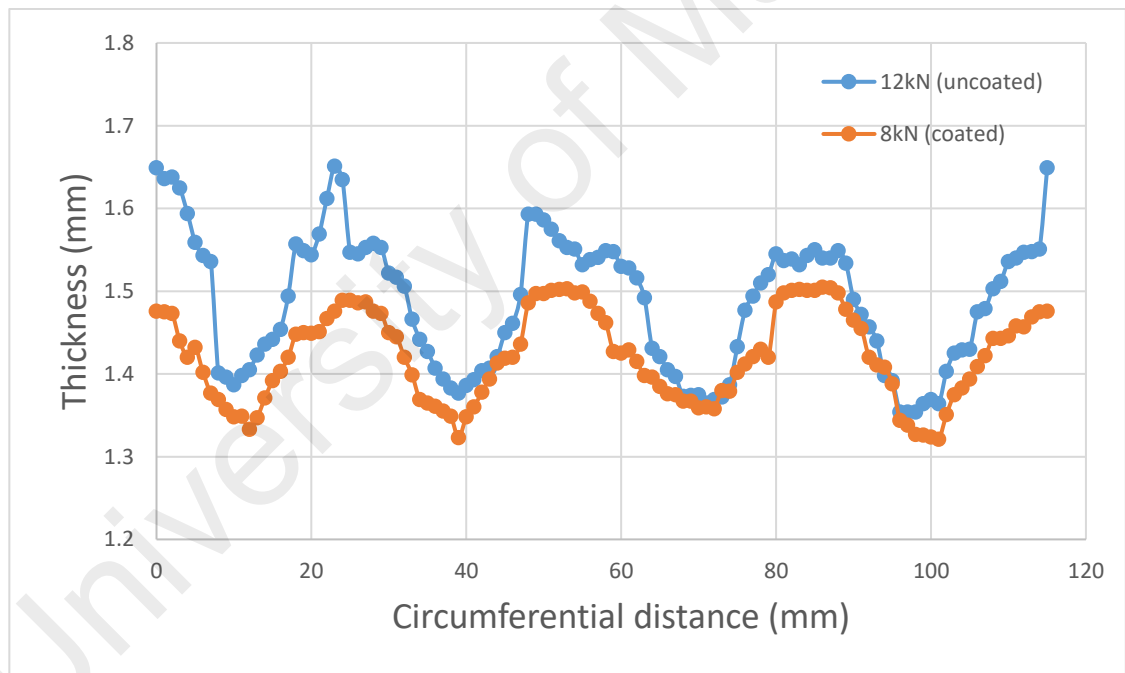
Figure 4.11: Change in wall thickness along the circumference direction

The change in wall thickness along circumference direction under the best performance BHF value 8kN and 12kN for both coated and uncoated die were shown in Figure 4.11. There was a significant drop in thickness when near the peak zone, while the increase of thickness could be found when near the valley zone. The deep-drawn cup form by TiN coated shows the lower amount of wall thickening at lower BHF compared to the uncoated die. This indicates the best performance of TiN coated die in aid the flow of material even the low BHF value was applied.

4.4   Residual Stress Measurement

The ring slitting results is shown in APPENDIX E. The tangential residual stresses measurement results with the ring slitting method for all crack-free drawn cups formed with both coated and uncoated die are shown in Table 4.8 and Figure 4.12.

Table 4.8: Ring slitting measurement results

5kN (coated die)				
Cup Height from Bottom	Ring Diameter (mm)	Ring Thickness (mm)	Ring-Opening distance (mm)	Residual Stress (MPa)
30%	33.31	1.00	1.66	82.61
60%	34.56	1.02	14.54	688.58
80%	34.72	1.17	12.04	659.86
100%	34.16	1.582	7.78	610.98
6kN (coated die)				
Cup Height from Bottom	Ring Diameter (mm)	Ring Thickness (mm)	Ring-Opening distance (mm)	Residual Stress (MPa)
30%	33.36	0.82	1.62	65.71
60%	34.11	1.14	14.12	768.37
80%	34.44	1.30	11.60	719.52
100%	34.04	1.574	7.72	607.52
7kN (coated die)				
Cup Height from Bottom	Ring Diameter (mm)	Ring Thickness (mm)	Ring-Opening distance (mm)	Residual Stress (MPa)

30%	33.34	1.02	2.30	120.25
60%	34.12	1.04	13.60	677.32
80%	34.46	1.10	11.22	589.76
100%	34.04	1.546	7.38	571.43

8kN (coated die)

Cup Height from Bottom	Ring Diameter (mm)	Ring Thickness (mm)	Ring-Opening distance (mm)	Residual Stress (MPa)
30%	33.34	1.02	1.62	81.83
60%	34.12	1.04	12.96	648.41
80%	34.46	1.10	11.48	602.36
100%	34.04	1.494	7.04	527.63

9kN (coated die)

Cup Height from Bottom	Ring Diameter (mm)	Ring Thickness (mm)	Ring-Opening distance (mm)	Residual Stress (MPa)
30%	33.60	0.90	2.68	122.96
60%	34.29	1.02	13.52	654.59
80%	34.39	1.18	11.46	647.63
100%	34.09	1.592	7.88	624.89

10kN (coated die)

Cup Height from Bottom	Ring Diameter (mm)	Ring Thickness (mm)	Ring-Opening distance (mm)	Residual Stress (MPa)
30%	33.40	1.02	4354	242.56
60%	34.44	1.08	13.46	684.64
80%	34.54	1.09	11.70	604.73
100%	33.74	1.586	7.62	617.98

12kN (Uncoated die)

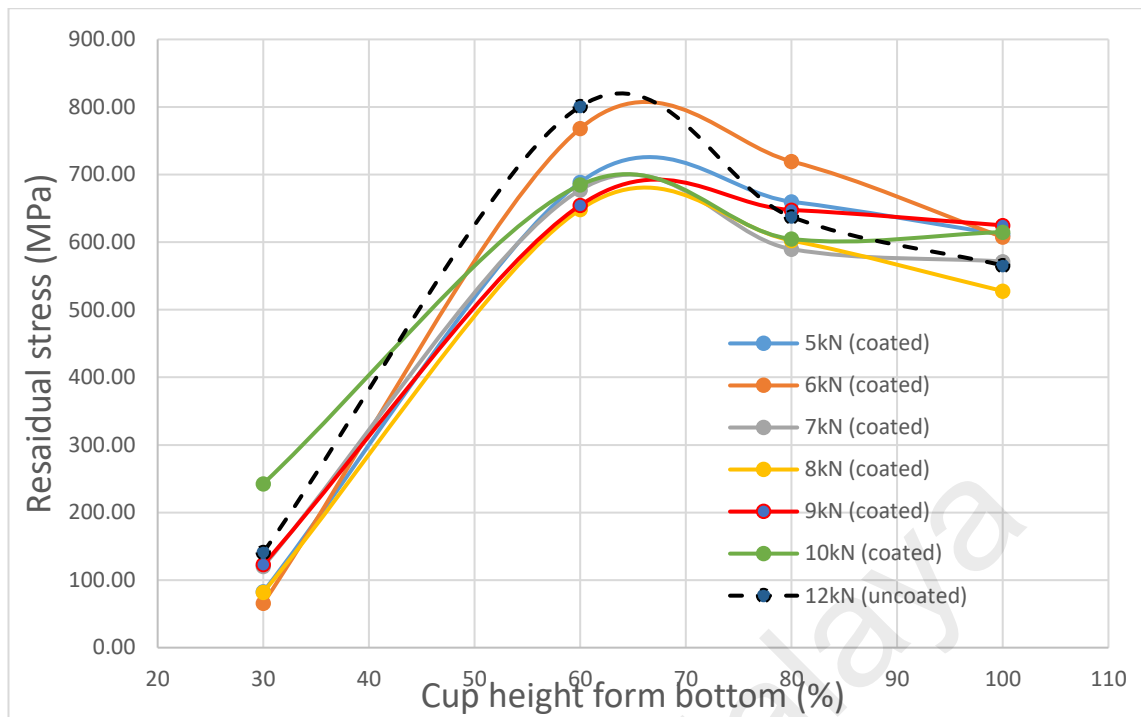| Cup Height from Bottom	Ring Diameter (mm)	Ring Thickness (mm)	Ring-Opening distance (mm)	Residual Stress (MPa)
30%	33.00	1.02	2.62	140.99
60%	34.002	1.12	15.00	800.79
80%	34.90	1.22	11.20	637.40
100%	34.30	1.537	7.46	565.63

Figure 4.12: Tangential residual stress

Residual stresses are induced in unstable austenitic stainless steels due to the inhomogeneous distribution of plastic strain and martensitic transformation. The residual stress for the crack-free deep drawn cup is shown in Figure 4.12. The open gap distance of the rings increased with height and was the largest at 60% height. The gap distance decreased with further increase in height. Therefore, the largest residual stress was obtained at 60% cup height. The stress reduced with a further increase in cup height up to 100% cup height.

At the flange portion which approximate 80 and 100% cup height was initially in contact with the blank holder and die before being pulled into the die cavity, the compression in this portion increased with BHF, resulting in greater deformation. In addition, the decreasing in area of contact between the punch and the blank during flange pulling will cause a pressure increase. Thus, the residual stress changes of 80% and 100% cup height were due to the increase of BHF acting on the flange during the drawing process.

Generally, the residual stress at 80% and 100% cup height reduced when the increase in BHF up to 8kN for TiN coated die. The reverse trend is observed for BHF greater 8kN, this might due to the increases of friction. The valley point has a higher risk for delayed crack, was located at 100% cup height, the reduced of the residual stress at this portion was favorable for eliminating or suppress the delayed cracks. In addition, the thinner wall thickness will lead to a lower residual stress. Theoretically, the magnitude of residual stresses in a deep drawn cup increase as deformation-induced martensitic transformation increases. As the coated die able lower the thickness along the cup edge thus reduce the concentration of deformation-induced martensite.

Chapter 5 CONCLUSION AND RECOMMENDATION

5.1   Conclusion

The successful cup forming BHF range for finely polished SKD-11 tool steel uncoated die was 6kN to 15kN. For the deep-drawn cup formed by the SKD-11 tool steel uncoated die, the only crack free BHF value was 12kN. The successful cup forming BHF range for TiN coated die was 5kN to 10kN; all cups formed within this BHF range are free from the delayed crack. The delayed-crack free BHF range for TiN coated die is larger than the finely polished SKD-11 tool steel uncoated die. The TiN-coated die has the largest delayed crack free BHF range at lower BHF compared to the uncoated die. The smaller value of BHF is always desired, due to the large value of the BHF will cause a higher risk for fracture at the cup bottom. In addition, no polishing is required for coated die after each drawing, die coating enhanced tool life and reduce the surface interactivity between the SUS304 blank and the die surface, resulting in the better surface finish of the product.

Theoretically, deformation-induced martensite increases with the amount of wall thickening. The delayed crack was most likely to occur at the valley point of the deep-drawn cup due to a large amount of wall thickening. Disappearance and reappearance of delayed cracks attributed to the amount of wall thickening in valley point and increases of valley height. The largest elongated valley reduces the amount of wall thickening and hence lowers the amount deformation-induced martensite. From the deep drawing test with the polished and uncoated die, a delayed crack appeared when the amount of wall thickening in valley point exceeded 33.5%. However, the cracks prevented for the amount of 28.0%. The lower ranges amount of wall thickening in valley point 24.5% - 32.7% were obtained from the deep drawing test with TiN coated die. The lower amount change in wall thickness in valley point and greater valley point height lead to delayed crack free cup form by TiN coated die. The smoother surface of TiN coated die (R_a=0.382µm) aid the flow of blank material into the die and largest elongation as possible.

The residual stresses can become very large for the deep drawing of austenitic stainless steel blank and cause the appearance of delayed crack. The maximum residual stresses can be found at the valley points, the delayed crack first appears and propagates from this point. Low residual stress at this 80 and 100% was favorable for eliminating delayed cracks. The deep-drawn cup formed by TiN coated die able to lower down the residual stress at 80% and 100% cup height due to the low wall thickness and concentration of deformation-induced martensite.

5.2   Recommendation

There are some recommendations for future related research. In order to clarify the performance of coated die in suppressing the delayed crack, different types of coated die such as TiC and DLC should be included. In addition, the delayed crack suppression effect of the coated die with applying less viscosity commercial lubricant should be included as well. For the residual stress measurement method, it should be including the other favors method X-ray diffraction method so that the accuracy of results can be ensured.

Due to the high cost for EDM cutting, the ring slitting testing was not performed on the cracked cups. As a result, the influence of the enhanced BHF on the residual stress distribution and the change in deformation behavior leading to the elimination of the delayed cracks remained unclear. Thus, it is necessary to include the ring slitting test for a cracked cup.

Theoretically, we know that the deep-drawn cup formed by coated will have the lower wall thickness in valley point and thus the low concentration of deformation-induced martensite. In order to verify this statement, it is important to include the analysis for the concentration of deformation-induced martensite on the deep drawn cup formed by coated die.

REFERENCES

Abe, Y., Ohmi, T., Mori, K., & Masuda, T. (2014). Improvement of formability in deep drawing of ultra-high strength steel sheets by coating of die. *Journal of Materials Processing Technology*, *214*(9), 1838–1843. https://doi.org/10.1016/j.jmatprotec.2014.03.023

Bak, S., Abro, M., & Lee, D. (2016). Effect of Hydrogen and Strain-Induced Martensite on Mechanical Properties of AISI 304 Stainless Steel. *Metals*, *6*(7), 169. https://doi.org/10.3390/met6070169

Berrahmoune, M. R., Berveiller, S., Inal, K., & Patoor, E. (2006). Delayed cracking in 301LN austenitic steel after deep drawing: Martensitic transformation and residual stress analysis. *Materials Science and Engineering A*, *438–440*(SPEC. ISS.), 262–266. https://doi.org/10.1016/j.msea.2006.02.189

Danckert, J. (1995). Reduction of the Residual Stresses in a Deep-Drawn Cup by Modifying the Draw Die Profile. *CIRP Annals - Manufacturing Technology*, *44*(1), 259–262. https://doi.org/10.1016/S0007-8506(07)62321-X

El Sherbiny, M., Zein, H., Abd-Rabou, M., & El shazly, M. (2014). Thinning and residual stresses of sheet metal in the deep drawing process. *Materials and Design*, *55*, 869–879. https://doi.org/10.1016/j.matdes.2013.10.055

Guo, X., & Bleck, W. (2016). Delayed Cracking in High Strength Steels, (August).

Huang, J. H., & Altstetter, C. J. (1991). Internal hydrogen-induced subcritical crack growth in austenitic stainless steels. *Metallurgical Transactions. A, Physical Metallurgy and Materials Science*, *22 A*(11), 2605–2618. https://doi.org/10.1007/BF02851354

Kala, A. (2017). The Effect of Process Parameters on Deep Drawing- A Review. *IJSRD - International Journal for Scientific Research & Development*.

Kim, S. H., Kim, S. H., & Huh, H. (2001). Finite element inverse analysis for the design of intermediate dies in multi-stage deep-drawing processes with large aspect ratio. *Journal of Materials Processing Technology*, *113*(1–3), 779–785. https://doi.org/10.1016/S0924-0136(01)00660-4

Kim, Y. H., Kim, K. Y., & Lee, Y. D. (2004). Nitrogen-Alloyed, Metastable Austenitic Stainless Steel for Automotive Structural Applications. *Materials and Manufacturing Processes*, *19*(1), 51–59. https://doi.org/10.1081/amp-120027498

Lo, K. H., Shek, C. H., & Lai, J. K. L. (2009). Recent developments in stainless steels. *Materials Science and Engineering R: Reports*, *65*(4–6), 39–104. https://doi.org/10.1016/j.mser.2009.03.001

Maksimkin, O. P. (1997). Deformation induced martensitic transformation in Cr-Ni stainless steel irradiated by neutrons. *Physica Status Solidi (A) Applied Research*, *163*(1). https://doi.org/10.1002/1521-396X(199709)163:1<R7::AID-PSSA99997>3.0.CO;2-T

Michler, T. (2015). Austenitic Stainless Steels. *Reference Module in Materials Science and Materials Engineering*, (June 2015), 1–6. https://doi.org/10.1016/b978-0-12-803581-8.02509-1

Murakawa, M. (1995). Ht#NOLOGY. *Surface and Coatings Technology*, *77*, 553–558.

Nilsson, J.-O. (2017). Retrieved from Stainless steel world magazine: http://www.stainless-steel-world.net/blogs/291/metastable-austenitic-stainless-steels.html

Papula, S., Saukkonen, T., Talonen, J., & Hänninen, H. (2015). Delayed Cracking of Metastable Austenitic Stainless Steels after Deep Drawing. *ISIJ International*, *55*(10), 2182–2188. https://doi.org/10.2355/isijinternational.isijint-2015-078

Papula, S., Talonen, J., & Hänninen, H. (2014). Effect of residual stress and strain-induced α′-martensite on delayed cracking of metastable austenitic stainless steels. *Metallurgical and Materials Transactions A: Physical Metallurgy and Materials Science*, *45*(3), 1238–1246. https://doi.org/10.1007/s11661-013-2090-3

Ragab, M. S., & Orban, H. Z. (2000). Effect of ironing on the residual stresses in deep drawn cups. *Journal of Materials Processing Technology*, *99*(1), 54–61. https://doi.org/10.1016/S0924-0136(99)00360-X

Swapna, D., Rao, C. S., & Radhika, S. (2018). A Review on Deep Drawing Process. *International Journal of Emerging Research in Management and Technology*, *6*(6), 146. https://doi.org/10.23956/ijermt.v6i6.260

Tajally, M., Emaddodin, E., & Qods, F. (2011). An experimental study on earing and planar anisotropy of low carbon steel sheets. *World Applied Sciences Journal*, *15*(1), 01–04.

Tan, C. J., & Aslian, A. (2019). FE simulation study of deep drawing process of SUS304 cups having no delayed cracks under enhanced blank holding force. *Proceedings of the Institution of Mechanical Engineers, Part B: Journal of Engineering Manufacture*, 1–11. https://doi.org/10.1177/0954405419855230

Tan, C. J., Ibrahim, M. S., & Muhamad, M. R. (2018). Preventing delayed cracks in SUS304 deep drawn cups using extreme blank holding forces aided by nanolubrication. *International Journal of Advanced Manufacturing Technology*. https://doi.org/10.1007/s00170-018-2772-5

Thye, Z.H. (2017). Experimental Study on Minimum Blank Holding Force for Eliminating Delayed Cracking In Deep Drawn SUS304 Cups Under Elevated Drawing Ratio.

Trzepieciński, T., & Gelgele, H. L. (2011). Investigation of anisotropy problems in sheet metal forming using finite element method. *International Journal of Material Forming*, *4*(4), 357–369. https://doi.org/10.1007/s12289-010-0994-7

Wu, Z., & Huang, Y. (2015). Characterization of a Metastable Austenitic Stainless Steel with Severe Plastic Distortions. *Procedia Engineering*, *99*, 1323–1329. https://doi.org/10.1016/j.proeng.2014.12.666

Zhang, S., & Zhu, W. (1993). TiN coating of tool steels: a review. *Journal of Materials Processing Tech.*, *39*(1–2), 165–177. https://doi.org/10.1016/0924-0136(93)90016-Y

Zinbi, A., & Bouchou, A. (2010). Delayed cracking in 301 austenitic steel after bending process: Martensitic transformation and hydrogen embrittlement analysis. *Engineering Failure Analysis*, *17*(5), 1028–1037. https://doi.org/10.1016/j.engfailanal.2009.11.007